

NEW INVARIANTS OF KNOTOIDS

NESLIHAN GÜĞÜMCÜ AND LOUIS H. KAUFFMAN

ABSTRACT. In this paper we construct new invariants of knotoids including the odd writhe, the parity bracket polynomial, the affine index polynomial and the arrow polynomial, and give an introduction to the theory of virtual knotoids. The invariants in this paper are defined for classical knotoids in analogy to corresponding invariants of virtual knots. The affine index polynomial and the arrow polynomial provide bounds on the height (minimum crossing distance between endpoints) of a classical knotoid. We show that classical knotoids have symmetric affine index polynomials.

1. INTRODUCTION

Knotoids are defined by V. Turaev in 2011 [34]. Knotoids in S^2 are open ended knot diagrams, forming a new diagrammatic theory that is an extension of the classical knot theory.

A standard 1-1 tangle (or long knot) has its endpoints in a single region of the diagram. A knotoid diagram generalizes the 1-1 tangle and allows the endpoints to be in different regions. This gives rise to a new theory and many new questions. Taking knotoids up to the equivalence described below, we can ask how far apart the endpoints need to be in all instances of diagrams for the equivalence class. We call this distance (in terms of crossing the boundaries of regions) the *height* of the knotoid. This sort of question about knotoids and their diagrams is a matter of combinatorial topology. Accordingly, we shall consider here a number of combinatorial topological invariants of knotoids, including the Jones polynomial.

We find that it is natural to examine knotoids in the context of virtual knot theory. Virtual knots are knots in thickened surfaces (or knot diagrams in surfaces) taken up to handle stabilization. There is a diagrammatic theory for virtual knots, as we explain in the body of the paper. It is natural to extend the notion of knotoids to virtual knotoids and to use ideas in virtual knot theory to construct new invariants of knotoids, including the knotoids defined in S^2 . Thus, we both extend knotoids to virtual knotoids and we use methods from virtual knot theory to study classical knotoids. This connection between classical knotoids and virtual knot theory is fundamental and will be the subject of work beyond the present paper. Classical knotoids are certainly a part of geometric three-dimensional knot theory and, as such, are related to open-ended embeddings of intervals in three dimensional space. We discuss this point of view as well in Section 2.1 of this paper. Many classical invariants

2010 *Mathematics Subject Classification.* 57M25, 57M27.

Key words and phrases. Knotoids, Virtual Knot, invariant, parity, flat diagrams, arrow polynomial, index polynomial, skein relation, bracket polynomial, height, lowerbound.

This research has been co-financed by the European Union (European Social Fund - ESF) and Greek national funds through the Operational Program "Education and Lifelong Learning" of the National Strategic Reference Framework (NSRF) - Research Funding Program: THALES: Reinforcement of the interdisciplinary and/or inter-institutional research and innovation.

of knots and links can be defined for knotoids, the fundamental group is a primary example. We concentrate on a combinatorial topological approach in the present paper and plan to consider more geometric approaches elsewhere.

One of the most remarkable conjectures arising from this paper is that the natural extension of the Jones polynomial to classical knotoids detects the unknot (in the category of knotoids). It appears to us that this conjecture has the same level of difficulty as the conjecture about knot-detection for the Jones polynomial of classical knots. This indicates the importance of knotoids for understanding the Jones polynomial and its relationship with geometric topology. We now summarize the contents of this paper.

The second section and the third section of this paper are recollections of classical knotoids, and virtual knot theory, respectively. In the second section we recall the basics of knotoids following V. Turaev's paper [34]. Then we give a geometric interpretation of classical knotoids as open oriented curves embedded in 3-dimensional space. Given an arbitrary oriented smooth open curve embedded in \mathbb{R}^3 we can project it to many planes, obtaining a multiplicity of knotoid diagrams in those planes. This collection of knotoids is a new measure (and definition) of the knottedness of an oriented smooth curve in space.

The third section continues with the presentation of virtual knotoids. Then we introduce flat virtual knotoid diagrams which will be a key ingredient for proving the theorems of the following sections. The third section ends with a discussion on the virtual closure map. The virtual closure determines a well-defined map from classical knotoids to virtual knots, so is a key to define invariants for knotoids via virtual knot invariants.

The fourth section is a discussion about parity for knotoids and introduces the odd writhe which is a simple and useful invariant of knotoids. Using the parity of knotoids, we re-define the parity bracket polynomial [24] for both classical and virtual knotoids. We show examples of nontrivial virtual knotoids whose non-triviality and also virtuality can be detected by the parity bracket polynomial. It is important to note that crossings of knotoids in S^2 can have parity. This is a remarkable appearance of parity in an essentially classical setting.

In the fifth section we define the affine index polynomial for knotoids, and prove its symmetry for classical knotoids. We show how the symmetry of the affine index polynomial can be used to detect virtuality of a virtual knotoid. Also we discuss the image of the virtual closure map by using the symmetry of the affine index polynomial.

In the sixth section we introduce the arrow polynomial and an extended version of the arrow polynomial for knotoids. We are already familiar with both the affine index and the arrow polynomial from virtual knot theory, and we show that they are nontrivial and useful invariants for knotoids as well. In both fifth and sixth sections, we show inequalities that relate these polynomials with the *height* (a minimal crossing distance between endpoints) of classical knotoids. These inequalities can often be used to determine the height of a knotoid.

We end the paper with a discussion of problems and directions for classical and virtual knotoids.

2. KNOTOIDS

Knotoid diagrams in S^2 are generic immersions of the unit interval $[0, 1]$ into S^2 endowed with over/under- crossing data at every transversal *crossing*, where the immersion is not 1-1. The images of 0 and 1 are distinct from each other, and from the crossings. These two points are the *endpoints* of a knotoid diagram and they are called the *tail* and the *head*, respectively. A projection of an open curve is *generic* if it is 1-1 at all points including the endpoints, except finitely many points where it is 2-1 and transversal in the sense that the tangent directions at the double point are distinct. A knotoid diagram can be seen as a generic projection of an open oriented curve embedded in $S^2 \times I$ to S^2 . Knotoid diagrams are oriented from the tail to the head. The trivial knotoid diagram is an embedding of the unit interval into S^2 . It is depicted by an arc without any crossings as shown in Figure 1a.

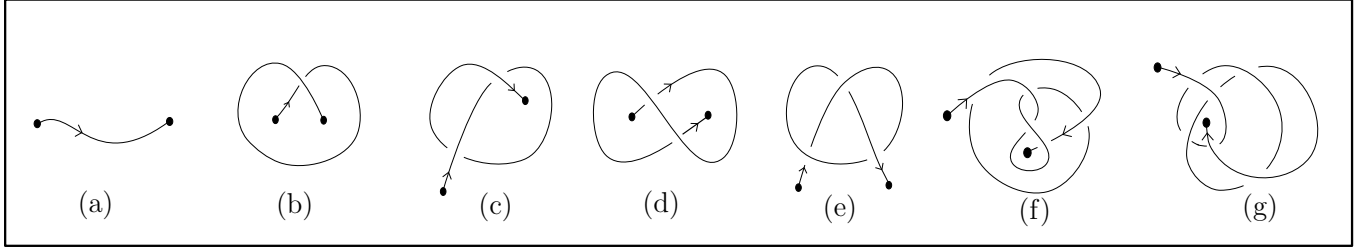
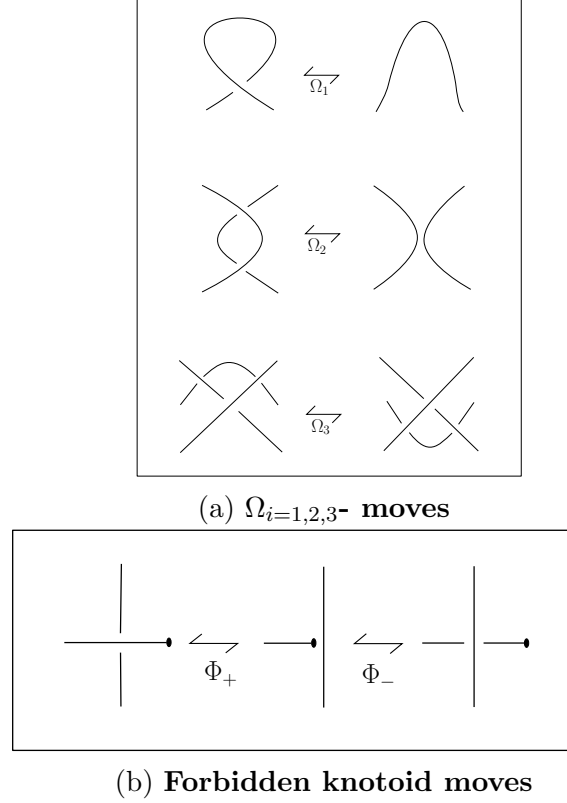


FIGURE 1. **Knotoid diagrams in S^2**

There are three Reidemeister moves on knotoid diagrams, Ω_1 , Ω_2 , Ω_3 . These moves modify a knotoid diagram within a small disk as shown in Figure 2a and they do not utilize the endpoints. It is forbidden to pull the strand adjacent to an endpoint over/under a transversal strand. These moves which are shown in Figure 2b, are called *forbidden knotoid moves*, and they are denoted by Φ_+ and Φ_- , respectively. If both Φ_+ and Φ_- moves are allowed, any knotoid diagram in S^2 can be turned into the trivial knotoid diagram.

FIGURE 2. The moves on knotoid diagrams in S^2

We call knotoid diagrams immersed in S^2 *classical knotoid diagrams*. The $\Omega_{i=1,2,3}$ -moves plus isotopy of S^2 generate an equivalence relation on classical knotoid diagrams. Two classical knotoid diagrams are said to be *equivalent* if they are related by a finite sequence of $\Omega_{i=1,2,3}$ -moves and isotopies of S^2 . A *classical knotoid* is an equivalence class of all equivalent classical knotoid diagrams. The set of classical knotoids is denoted by $K(S^2)$, comprises all classical knotoids.

Definition 1. Let \mathcal{M} be a category of mathematical structures (e.g. polynomials, Laurent polynomials, the integers modulo five, commutative rings, groups, \dots). An *invariant* of classical knotoids is a mapping $I : \text{Classical Knotoids} \rightarrow \mathcal{M}$ such that equivalent knotoids map to equivalent structures in \mathcal{M} .

Every classical knotoid diagram represents at least one classical knot in 3-dimensional space. One way to obtain a classical knot diagram from a given knotoid diagram K in S^2 is to connect the endpoints of K by an embedded arc in S^2 which is declared to go under each strand it meets during the connection. Therefore we have a classical knot diagram in S^2 representing a knot in 3-dimensional space. We call an embedded arc connecting the endpoints a *shortcut* of K . This way of connecting the endpoints of a classical knotoid diagram is called *underpass closure*. Up to isotopy, there is a unique shortcut for every classical knotoid diagram. The isotopy between any two shortcuts induces isotopy between the resulting classical knots, so any of shortcuts gives the same isotopy class of classical knots. It is not hard to see that the underpass closure respects the equivalence classes of classical

knotoids. In fact, any $\Omega_{i=1,2,3}$ -move between two equivalent classical knotoid diagrams is transformed to Reidemeister moves between the corresponding knot diagrams obtained by the underpass closure. Therefore, the underpass closure defines a well-defined map denoted by ω_- ,

$$\omega_-: \text{Classical Knotoids} \rightarrow \text{Knots in } \mathbb{R}^3.$$

Every classical knot can be represented by a classical knotoid diagram. We take an oriented diagram of the knot, κ in S^2 and cut out an open arc from the diagram that contains no crossing or one or more overcrossings from the diagram so that we have a knotoid diagram representing κ . Note that all such knotoid diagrams will go back to κ by the underpass closure. This way we obtain a number of classical knotoid diagrams which may be nonequivalent to each other depending on the arc we cut, but they all represent the same classical knot. The knotoid diagrams may have fewer crossings than the crossings of any knot diagram of the knot. Such a representation is advantageous for computation of many knot invariants like the knot group or the Seifert genus [34]. Exploring properties of the knotoids representing the same knot is an interesting task in knotoid theory.

One other way to obtain a classical knot diagram from a given classical knotoid diagram is to connect the endpoints of the knotoid diagram with an embedded arc in S^2 which goes over each strand it meets during the connection. This operation is called *overpass closure* of knotoid diagrams. The overpass closure also defines a well-defined map from the set of classical knotoids to the set of classical knots. Thus the overpass closure of a classical knotoid diagram determines a unique classical knot. The overpass closure and the underpass closure of a classical knotoid diagram can give rise to non-isotopic knots. For instance, the overpass closure of the knotoid diagram in Figure 1c is the trivial knot but the underpass closure gives a trefoil. To have a well-defined representation of a classical knot via classical knotoids, we fix the connection type as either the overpass or the underpass closure.

The theory of classical knotoids extends classical knot theory. In fact, there is a well-defined injective map,

$$\alpha: \text{Classical Knot Diagrams in } S^2 / \langle R1, R2, R3 \rangle \rightarrow \text{Classical Knotoids}$$

where $R1, R2, R3$ are the usual Reidemeister moves and for D is an oriented knot diagram in S^2 , the map α is defined by cutting out an open arc of D which is apart from the crossings of D . The resulting diagram is a knotoid diagram in S^2 with two endpoints in the same local region of the 2-sphere. The classical knotoid represented by this knotoid diagram does not depend on the arc that is cut out from the knot diagram: Let a be an open arc of the diagram D , instead of cutting a , we can pull a along D under or over the crossings and then cut that arc. This pulling of the arc transforms as Ω_i -moves, $i = 1, 2, 3$, on the resulting knotoid diagrams. It is not hard to see that the map α respects the equivalence classes of knot diagrams. For injectivity, it is sufficient to see that both underpass and overpass closures of any classical knotoid which is in the image of α give equivalent knot diagrams.

Classical knotoids which are in the image of the α map are called *knot-type knotoids* and classical knotoids which are not in the image are called *pure* or *proper knotoids* (we shall say proper). Any knot-type knotoid has a knotoid diagram in its equivalence class with endpoints in the same local region of the 2-sphere. Such a diagram is called a *knot-type knotoid diagram*. The endpoints of a proper knotoid can be in any local but different regions

of S^2 for any representative diagram. In Figure 1e we see a knot-type knotoid diagram; all the other knotoid diagrams in Figure 1 are proper knotoid diagrams. The set of knotoids, $\mathcal{K}(S^2)$ can be regarded as the union of all knot-type and proper knotoids. Classical knots embed into this set as knot-type knotoids. Note that a knot-type knotoid can be thought as a $1 - 1$ tangle or a long knot. It is well-known that a classical long knot carries the same knotting information as the classical knot obtained by closing the two endpoints of the long knot [5, 20, 25, 35]. It is immediate that a knot-type knotoid can be considered the same as the classical knot it represents via the ω_- -map. For proper knotoids this is no longer true. There are nontrivial proper knotoids representing the trivial knot. The knotoid given by the diagram in Figure 1d is a nontrivial proper knotoid [34] but it represents the trivial knot. It is one of the fundamental problems in our paper to determine the type of a given classical knotoid.

A classical knotoid diagram can be also defined to be an immersion of the unit interval into \mathbb{R}^2 . The equivalence on planar knotoid diagrams is given by the same three Reidemeister moves that are away from the endpoints and ambient isotopy of \mathbb{R}^2 . The set of all planar classical knotoids comprises all equivalence classes of classical knotoid diagrams in \mathbb{R}^2 and denoted by $\mathcal{K}(\mathbb{R}^2)$. In fact, we usually draw knotoid diagrams which are defined in S^2 , to the plane. For this reason it is worth comparing the two sets, $\mathcal{K}(S^2)$ and $\mathcal{K}(\mathbb{R}^2)$. There is an inclusion map

$$\iota : \mathcal{K}(\mathbb{R}^2) \rightarrow \mathcal{K}(S^2)$$

which is induced by the inclusion $\mathbb{R}^2 \hookrightarrow S^2$. Any classical knotoid in S^2 can be represented by a knotoid diagram in \mathbb{R}^2 by pushing a representative diagram in the 2-sphere away from the $\infty \in S^2$. Considering the equivalence class of this planar representation in $\mathcal{K}(\mathbb{R}^2)$, there is a well-defined map $\rho : \mathcal{K}(S^2) \rightarrow \mathcal{K}(\mathbb{R}^2)$. It is clear that $\iota \circ \rho = id$ so that ι is surjective. There are examples of nontrivial classical knotoids in \mathbb{R}^2 which are trivial in $\mathcal{K}(S^2)$. The simplest example for this is the given diagram in Figure 1b which represents a nontrivial planar knotoid [34] but represents the trivial knotoid in the 2-sphere. Thus the map ι is not injective. In this paper, we study mostly the classical knotoids in S^2 and we mean classical knotoids in S^2 unless otherwise stated.

Definition 2. *Multi-knotoid diagrams* are defined as generic immersions of the oriented unit interval and several oriented circles into S^2 with finitely many double points endowed with the under/over data. So a multi-knotoid diagram consists of a knotoid component and several closed components. The equivalence relation on knotoid diagrams in S^2 extends to an equivalence relation on multi-knotoid diagrams and a *multi-knotoid* is defined to be the equivalence class of a multi-knotoid diagram. Many of the invariants discussed in this paper extend to multi-knotoids. We will remark on this as the paper proceeds.

2.1. An Interpretation of Classical Knotoids in 3-Dimensional Space. Let K be a classical knotoid diagram in \mathbb{R}^2 . The plane of the diagram is identified with $\mathbb{R}^2 \times \{0\} \subset \mathbb{R}^3$. K can be embedded into \mathbb{R}^3 by pushing the overpasses of the diagram into the upper half-space and the underpasses into the lower half-space. The tail and the head of the diagram are attached to the two lines, $t \times \mathbb{R}$ and $h \times \mathbb{R}$ that pass through the tail and the head, respectively and perpendicular to the plane of the diagram. Moving the endpoints of K along these special

lines gives rise to embedded open oriented curves in \mathbb{R}^3 with two endpoints of each on these lines.

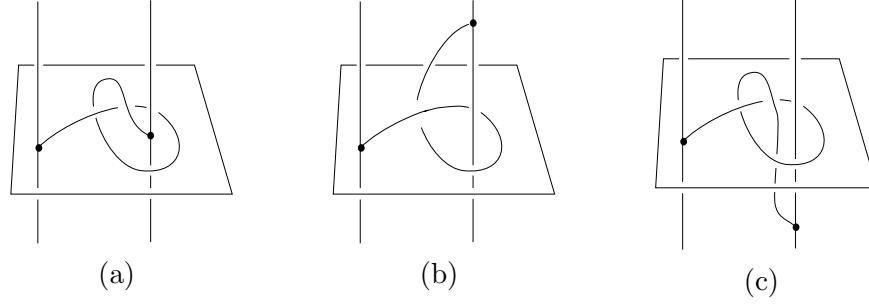


FIGURE 3. Curves in \mathbb{R}^3 obtained by the knotoid diagram in Figure 1c

Two smooth open oriented curves embedded in \mathbb{R}^3 with the endpoints that are attached to two special lines, are said to be *line isotopic* if there is a smooth ambient isotopy of the pair $(\mathbb{R}^3 \setminus \{t \times \mathbb{R}, h \times \mathbb{R}\}, t \times \mathbb{R} \cup h \times \mathbb{R})$, taking one curve to the other curve in the complement of the lines, taking endpoints to endpoints, and taking lines to lines; $t \times \mathbb{R}$ to $t \times \mathbb{R}$ and $h \times \mathbb{R}$ to $h \times \mathbb{R}$. The curves given in Figure 3 are line isotopic to each other.

Conversely, let be given an open oriented embedded curve in \mathbb{R}^3 with a generic projection to the xy - plane. The endpoints of the curve determine two lines passing through the endpoints and perpendicular to the plane. The generic projection of the curve to the xy - plane along the lines which is endowed with over and under-crossing data, is a knotoid diagram in \mathbb{R}^2 . We call a smooth open embedded curve in \mathbb{R}^3 that has a generic projection to the xy - plane a *generic curve with respect to the xy -plane*. Such a curve has a line isotopy class as described in the previous paragraph.

Theorem 2.1. *Two smooth open oriented curves in \mathbb{R}^3 that are generic with respect to the xy -plane are line isotopic with respect to the lines passing through the endpoints if and only if their generic projections to the xy -plane (along the lines) are equivalent classical knotoid diagrams, that is, they are related by $\Omega_{i=1,2,3}$ - moves and isotopy of the plane.*

Proof. Since everything is set in the smooth category, we can switch to the piecewise linear category. Open curves are defined as *piecewise linear curves* in \mathbb{R}^3 , that is, as the union of finitely many edges: $[p_1, p_2], \dots, [p_{n-1}, p_n]$ such that each edge intersects one or two other edges at the points, p_i , $i = 2, \dots, n-1$ and p_1 and p_n are the endpoints of the curve. We define the *triangle move* in 3- dimensional space. Given an open curve with endpoints on the lines, let $[p_i, p_{i+1}]$ be an edge of the curve and p_0 be a point in the complement of the curve and the two lines. The edge is transformed to two edges $[p_i, p_0]$ and $[p_0, p_{i+1}]$ which form a triangle, whenever this triangle is not pierced by another edge of the curve or by the lines. In the reverse direction, a consecutive sequence of two edges may be transformed to one edge by a triangle move. An ambient isotopy of a piecewise linear curve in the complement of the two lines can be expressed by a finite sequence of triangle moves.

By using triangle moves we can subdivide the edges into smaller edges as shown in Figure 4. Any triangle move can be factored into a sequence of smaller triangular moves by *subdividing* the triangles and the edges accordingly. Consider the projection of a curve to the plane, triangular regions that triangular moves take place are projected to non-singular triangles

and these triangles possibly contain many strands which are the projection of other edges. The entire ambient isotopy of the curve can be reduced to the shadow cases in the plane shown in Figure 5, by subdivision. Inducting on the strands inside the triangles shows that triangle moves are generated by $\Omega_{i=1,2,3^-}$ moves, shown in the left of the figure and the right side shows some cases that are combinations of $\Omega_{i=1,2,3^-}$ moves. \square

Corollary 2.1. *There is a one-to-one correspondence between the set of classical knotoids in \mathbb{R}^2 and the set of line-isotopy classes of smooth open oriented curves in \mathbb{R}^3 with two endpoints attached to lines that pass through the endpoints and perpendicular to the xy -axis.*

It may be the case that a smooth open oriented curve embedded in \mathbb{R}^3 is not generic with respect to the xy -plane but can be generic with respect to many other planes. Projecting the curve generically to these planes gives a set of knotoid diagrams immersed in the planes. The line isotopy can be generalized to all the curves that is generic with respect to some plane and the theorem above generalizes as follows.

Theorem 2.2. *Two open oriented curves embedded in \mathbb{R}^3 that are both generic to a given plane, are line isotopic (with respect to the lines determined by the endpoints of the curves and the plane) if and only if the projections of the curves to that plane are equivalent classical knotoid diagrams in the plane.*

We say that a knotoid in a plane *represents* an open oriented embedded curve in \mathbb{R}^3 if the knotoid is in the equivalence class of the generic projection of the curve to some plane.

The equivalence classes of classical knotoids in the planes all representing the same open curve embedded in 3-dimensional space, can vary with respect to the projection plane. For instance, the projection of the curve represented in Figure 3b to the yz -plane gives a knotoid diagram with the tail and the head in the unbounded region of the plane and one can see that it is equivalent to the trivial knotoid in the yz -plane. The projection to the xy -plane, however, is the knotoid diagram given in Figure 1c and we will show in Section 3.3 that this knotoid is a nontrivial classical knotoid in S^2 so is nontrivial in \mathbb{R}^2 .

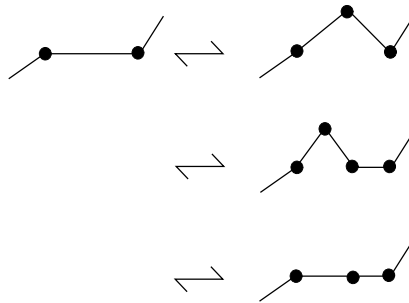
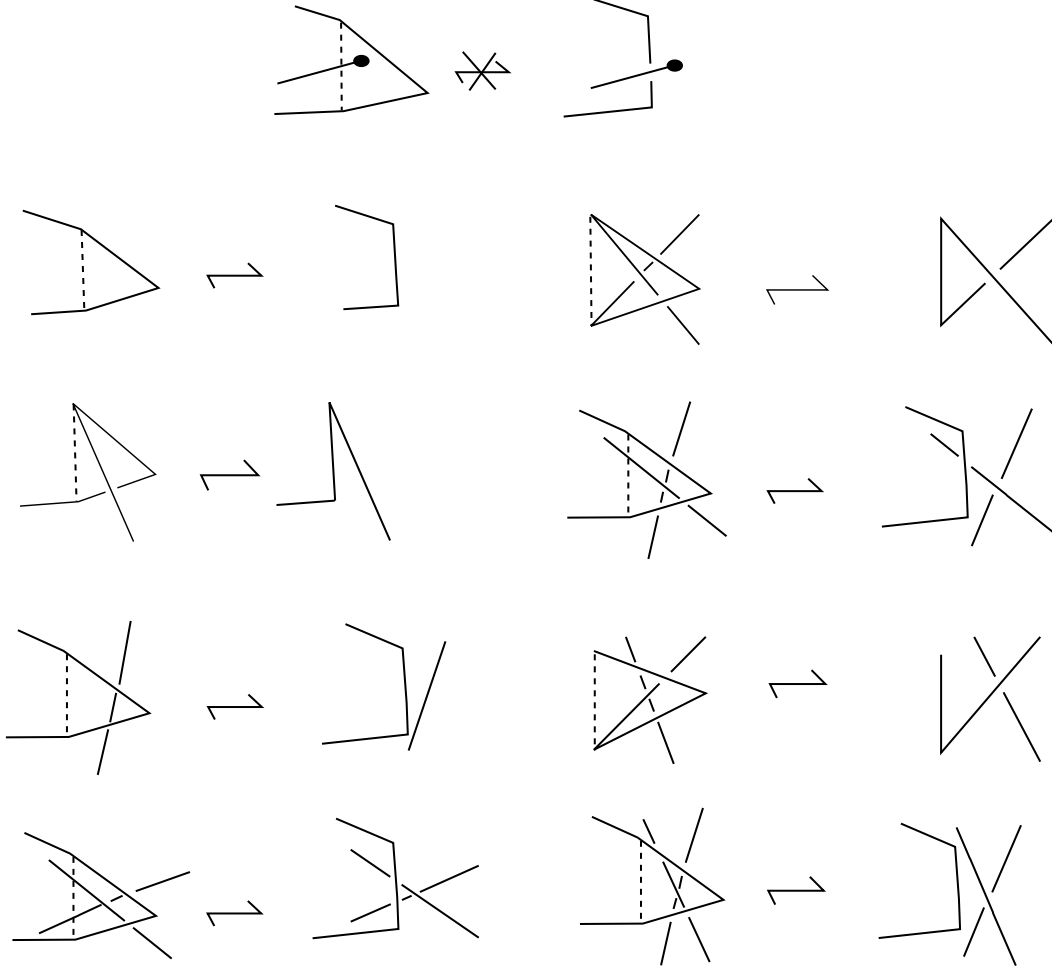


FIGURE 4. Subdivision of an edge

FIGURE 5. **Shadow of triangular moves**

Given a smooth open oriented curve embedding C in \mathbb{R}^3 , we define $\mathcal{P}(C)$ to be the set of all classical knotoid equivalence classes obtained from generic projection of C to planes in \mathbb{R}^3 that are outside a ball containing C . We take $\mathcal{P}(C)$ as a measure of the knottedness of C . Each knotoid in $\mathcal{P}(C)$ can represent three knots; two classical knots via the underpass and overpass closures, and a virtual knot with genus at most 1 via the virtual closure, see Section 3.3 for the definition of virtual closure. The set of knots that are represented by knotoids in $\mathcal{P}(C)$ can be used as possible closures of C . This is a new way to measure the knottedness of an open curve and may have significant applications in the study of tangled physical systems. The reader should compare our definition with the work of [6].

Figure 6 shows a semi-realistic picture of an open curve in space depicting a bowline knot and a possible closure of that knot. This same picture can be viewed (by making the lines more abstract) as a knotoid projection of the bowline. The right-hand picture is the underpass closure of this knotoid that is an 8 crossings classical knot. On the other hand, the overpass closure is a classical knot with 6 crossings. The interested reader is encouraged to find the corresponding classical knots in the knot table [23]. Moreover the virtual closure of this knotoid is a nontrivial, genus 1 virtual knot. We suggest that a collection of closures

of an open curve in space can be obtained by considering both underpass and overpass and also virtual closures of all the generic knotoid projections of the given open curve.

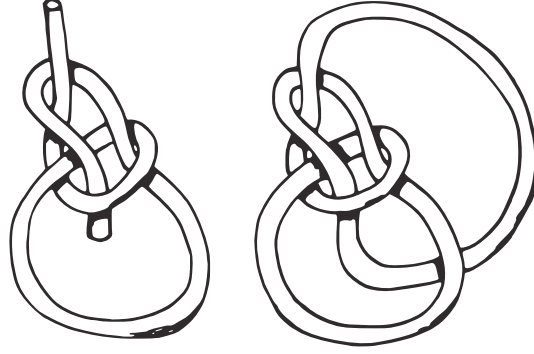


FIGURE 6. A closure of bowline knot projection

3. VIRTUAL KNOTS AND VIRTUAL KNOTOIDS

The theory of virtual knots, introduced by L.H. Kauffman [12,13] in 1996, studies the embeddings of circles in thickened surfaces modulo isotopies and diffeomorphisms of the surface and one-handle stabilization of the surfaces. Virtual knot theory has a diagrammatic formulation. In the diagrammatic theory, virtual knots and links are represented by diagrams with finitely many transversal crossings which are called *classical* or *real* crossings and there is another type of crossing called a *virtual* crossing which is neither an over-crossing nor an under-crossing. A virtual crossing is an artifact of the representation of the virtual knot diagram in the plane (or equivalently in S^2) and it is indicated by two crossing segments with a small circle placed around the crossing point.

The moves on virtual diagrams are generated by the usual Reidemeister moves plus the detour move. The detour move allows a segment with a consecutive sequence of virtual crossings to be excised and replaced any other such a segment with a consecutive virtual crossings, as seen in Figure 7a. Virtual knot and link diagrams that can be connected by a finite sequence of these moves are said to be *equivalent* or *virtually isotopic*.

Virtual knots and links can also be represented by embeddings without any virtual crossings in thickened orientable surfaces just as non-planar graphs may be embedded in surfaces of some genus. There is a unique abstract knot/link diagram assigned to each virtual knot/link diagram. Abstract knot/link diagrams are associated to thickened closed connected orientable surfaces in which the knot diagram is embedded. The details on abstract diagrams and their association with thickened surfaces will be given in the next section. Here we state the following theorem.

Theorem 3.1. (*[2, 12, 14, 15]*) *Two virtual link diagrams are virtually isotopic if and only if their surface embeddings are equivalent up to isotopy and diffeomorphism of the surface, and addition/removal of empty handles.*

3.1. Virtual Knotoids. We extend classical knotoid diagrams to virtual knotoid diagrams in a combinatorial way. *Virtual knotoid diagrams* are defined to be the knotoid diagrams

in S^2 with an extra combinatorial structure called *virtual crossings* that are indicated by a circle around the crossing point as in the case of virtual knots. Figure 11 depicts an example of a virtual knotoid diagram. The moves on virtual knotoid diagrams are generated by the $\Omega_{i=1,2,3}$ -moves and the detour move. One special case of the detour move is Ω -virtual move denoted by Ω_v , which enables to slide back/forth the strand which is adjacent to the tail or the head and having consecutive virtual crossings. The Ω_v - move decreases or increases the number of virtual crossings by 1 and change the locations of the endpoints. Figure 7b and Figure 7c depict all special cases of the detour move. These moves together with the $\Omega_{i=1,2,3}$ -moves are called *generalized Ω -moves*.

The generalized Ω - moves define an equivalence relation on virtual knotoid diagrams. We say that two virtual knotoid diagrams are *virtually equivalent* if one can be obtained from the other by a finite sequence of the generalized Ω -moves and isotopies of S^2 . A *virtual knotoid* is an equivalence class of all virtually equivalent virtual knotoid diagrams.

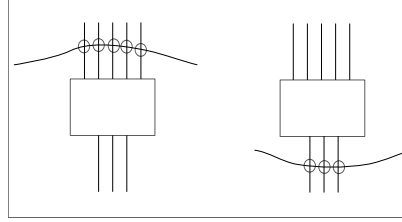
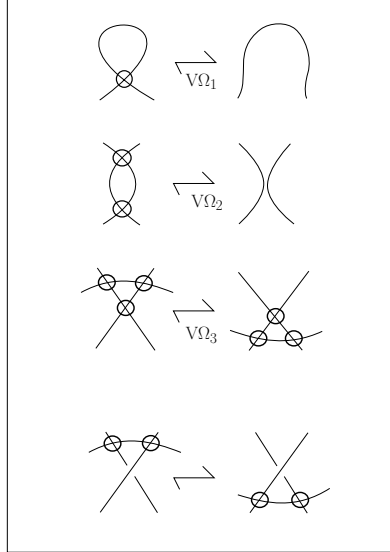
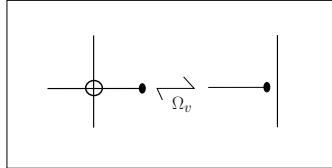
(a) **The detour move**(b) **Virtual $\Omega_{i=1,2,3}$ -moves and the partial virtual move**(c) **Ω -virtual move**

FIGURE 7. Moves on virtual knotoid diagrams

There are two more moves on virtual knotoid diagrams shown in Figure 8 which resemble the Reidemeister moves but are not resulted from any of the classical $\Omega_{i=1,2,3}$ -moves or the detour move. We call them *virtual forbidden moves*. The virtual forbidden moves slide either an underpassing or overpassing under/over a virtual crossing and they are denoted by Φ_{under} and Φ_{over} , respectively. These moves are also forbidden moves for the closed virtual knots/links. Together with the generalized Reidemeister moves these forbidden moves trivialize the theory of virtual knots [29]. And in the same way, the virtual forbidden moves trivialize the theory of virtual knotoids. By observing the effect of the virtual forbidden moves on the corresponding chord diagrams of knotoid diagrams (see Section 4.1 for the chord diagrams), we can show that any virtual knotoid diagram can be transformed to the trivial knotoid diagram. The utilization of only the over-forbidden move, Φ_{over} yields a nontrivial theory called *welded knot theory* [12, 32]. We define the corresponding *welded knotoid theory*.

Definition 3. Two virtual knotoid diagrams are said to be *w-equivalent* if they can be obtained from one another by a sequence of the generalized Ω -moves, the over-forbidden move, Φ_{over} and the Φ_- -move (see Figure 2b). The corresponding equivalence classes are called *welded virtual knotoids*.

S. Satoh in his paper [33] defines *w-equivalence* on virtual knotoid diagrams (named as *virtual arc diagrams* in the paper) just in the same way. He shows that any two w-equivalent virtual knotoid diagrams present equivalent ribbon 2-knots in \mathbb{R}^4 and the fundamental group of the complement of any ribbon 2-knot is isomorphic to the fundamental group of the associated welded virtual knotoid. The fundamental group of a virtual knotoid diagram is given by the generators associated to the overpasses of the diagram and at each classical crossing there is a relation defined in the same way with the relations of Wirtinger presentation. Note that the fundamental group of any classical knotoid diagram K is invariant under the three Reidemeister moves and the Φ_- -move and it is isomorphic to the fundamental group of the classical knot given by the underpass closure of K , see [34] and [33] in which it is given in terms of w-equivalences of classical arc diagrams.

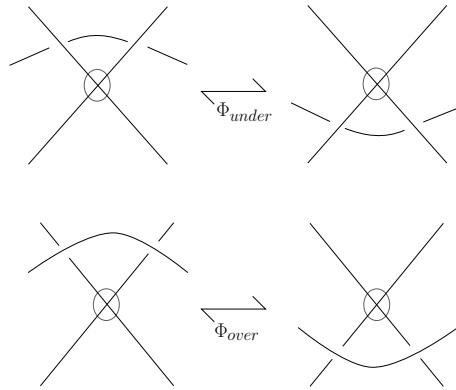


FIGURE 8. Virtual forbidden moves

Definition 4. Let \mathcal{M} be a category of mathematical structures. A virtual knotoid invariant is a mapping $I: \text{Virtual Knotoids} \rightarrow \mathcal{M}$ such that virtually equivalent knotoids map to equivalent structures in \mathcal{M} .

As with virtual knots, the theory of virtual knotoids has a topological interpretation. Knotoid diagrams can be defined in higher genus, closed, connected, orientable surfaces as generic immersions of the unit interval, with two distinct endpoints as the images of 0 and 1. Unless otherwise indicated, a surface will mean a closed, connected, orientable surface throughout the paper. The following theorem was stated by V. Turaev in his paper [34] as a remark. Here we give a proof of that remark.

Theorem 3.2. *The theory of virtual knotoids is equivalent to the theory of knotoid diagrams in higher genus surfaces considered up to isotopy in the surface, diffeomorphisms of the surface and addition/removal of handles in the complement of knotoid diagrams.*

Proof. The proof will follow similarly with the proof of Theorem 3.1. We first introduce abstract knotoid diagrams that form a middle stage for the proof.

Let K be a virtual knotoid diagram, an *abstract knotoid diagram* associated to K , (F, K) is a ribbon-neighborhood surface, obtained by attaching a 2-disc to each classical crossing and to the two endpoints of K such that the crossings and the endpoints are contained in the discs and these discs are connected by ribbons. The virtual crossings are represented by ribbons that pass over one another as depicted in Figure 9b. The abstract knotoid diagrams are pictured as embedded in 3-dimensional space, but we do not consider a particular embedding. Thus to every virtual knotoid diagram there is a uniquely associated abstract knotoid diagram.

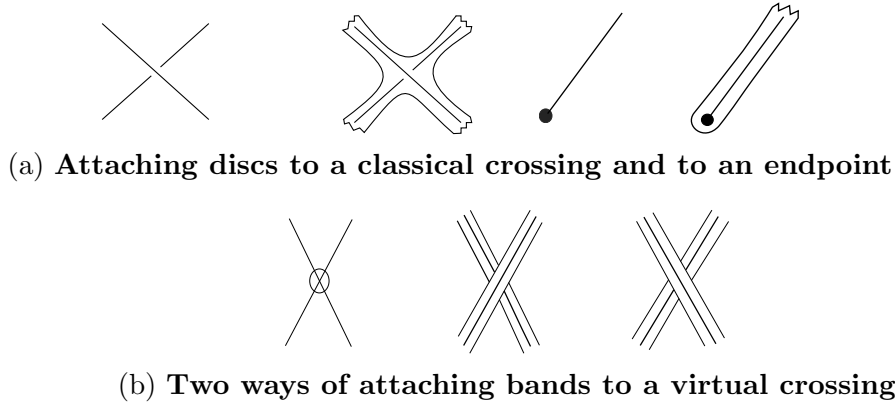
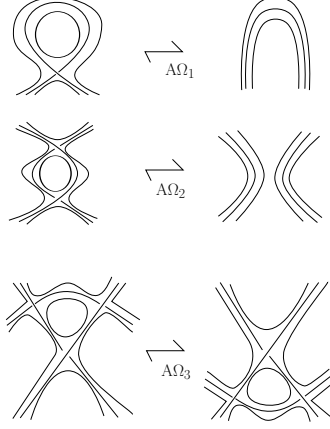


FIGURE 9

We say that two abstract knotoid diagrams are *abstractly equivalent* if two can be obtained from one another by finitely many *abstract Ω -moves*. These moves are ribbon versions of the generalized Ω -moves which are accomplished by closing the surface with a disc and applying an isotopy in the surface. The ribbon detour moves are accomplished by just moving one of the non-intersecting free ribbon bands. An *abstract knotoid* is the equivalence class of all abstractly equivalent abstract knotoid diagrams.

FIGURE 10. Abstract Ω -moves

Proposition 3.3. *The mapping*

$$\Phi: \text{Virtual Knotoid Diagrams} \rightarrow \text{Abstract Knotoid Diagrams}$$

explained above induces a bijection

$$\Phi_*: \text{Virtual Knotoid Diagrams/virtual eqv.} \rightarrow \text{Abstract Knotoid Diagrams/abstract eqv.}$$

Proof. Let K_1, K_2 be two virtually equivalent knotoid diagrams. The generalized Ω -moves transform to abstract knotoid moves between $\Phi_*(K_1)$ and $\Phi_*(K_2)$. This shows the map Φ_* is well-defined.

There exists a map from the set of abstract knotoids to the set of virtual knotoids, defined by projecting an abstract diagram which is embedded in S^3 in such a way that the 2-disks containing the classical crossings and the endpoints lie in $S^2 \subset S^3$. The segments through transversal ribbon bands project as transversal segments forming a virtual crossing thus this embedding projects onto S^2 as a virtual knotoid diagram. It is easy to check that this map is well-defined and forms the inverse of Φ_* . This completes the proof of Proposition 3.3. \square

Abstract knotoid diagrams are also associated to knotoids in surfaces of higher genus in the following sense. The abstract knotoid diagram (F, K) associated to a virtual knotoid diagram K is a compact surface with boundary. Let $\Gamma(K)$ be the underlying graph of K . This graph is connected and has n four-valent vertices corresponding to classical crossings of K and two one-valent vertices corresponding to the endpoints of K , and $\Gamma(K)$ has $2n + 1$ edges. (F, K) deformation retracts to $\Gamma(K)$. We close the boundary components of (F, K) with 2-disks to have a representation of the virtual knotoid K in a closed oriented surface of genus g ,

$$g = 1 + ((n - 1) - \delta)/2,$$

where n is the number of classical crossings of K and δ is the number of boundary components of (F, K) .

This closed surface of genus g , $\overline{(F, K)}$ is the least genus surface among the surfaces in which that knotoid diagram K can be immersed without any virtual crossings. We can add empty handles to this surface to increase the genus so that K is represented in other surfaces

without any virtual crossings. On the other hand, given a knotoid diagram K in a surface of genus \tilde{g} , $\Sigma_{\tilde{g}}$, the regular neighborhood of the diagram $(N(K), K)$ can be regarded as an abstract knotoid diagram. If the complement of $(N(K), K) \subset \Sigma_{\tilde{g}}$ has genus g , we can cut out this extra genus to reduce the genus of the surface to the genus of the disk-closure of the abstract knotoid diagram of K , (\overline{F}, K) .

Let K_1, K_2 be two knotoid diagrams in surfaces Σ_1, Σ_2 , respectively. (Σ_1, K_1) and (Σ_2, K_2) are said to be *stably equivalent* if one is obtained from the other by isotopy of the surfaces, diffeomorphisms of the surfaces and the addition/subtraction of empty handles in the complement of the diagrams.

Proposition 3.4. *The mapping*

$\Psi: \text{Abstract Knotoid Diagrams} \rightarrow \text{Knotoid Diagrams in Surfaces of genus } g$
defined by assigning (F, K) to (\overline{F}, K) induces a bijection

$\Psi_*: \text{Abstract Knotoid Diagrams/abstract eqv.} \rightarrow \text{Knotoid Diagrams in Surfaces/stable eqv.}$

Proof. The map Ψ_* is well-defined since the abstract Ω -moves between two equivalent abstract knotoid diagrams correspond to stable equivalence of the corresponding surface diagrams. In fact, filling the boundaries of abstract knotoid diagrams with 2-disks, abstract Ω_1 and Ω_3 -moves transform to Ω_1 - and Ω_3 -moves between the knotoid diagrams represented in surfaces of the same genus. The genus does not change under these two moves. The genus of the associated surface is not invariant under an abstract Ω_2 -move. This move may increase/decrease the genus of the surface by 1. In the case of genus change, the abstract Ω_2 -move corresponds to Ω_2 -move plus destabilization (removal of empty handles) in the associated surface.

Let K be a knotoid diagram in a surface Σ_g . The regular neighborhood of the diagram in Σ_g is an abstract knotoid diagram whose closure with 2-disks is stably equivalent to (Σ_g, K) . So, the map is surjective. It is not hard to see that stable equivalence induces abstract equivalence between the corresponding abstract knotoid diagrams, so the map is also injective. This completes the proof of Proposition 3.4. \square

The composition of the two bijections Φ_* and Ψ_* gives the needed bijection between the virtual knotoids defined up to virtual equivalence and knotoids in higher genus surfaces defined up to the stable equivalence. This completes the proof of Theorem 3.2. \square

Projecting a knotoid diagram that lies in a higher genus surface to S^2 results in virtual crossings. We make this projection canonical by forming the abstract diagram in the surface and then arranging a standard projection of the abstract diagram. Figure 11 depicts the projection process.

The *genus* of a knotoid is the least genus among the surfaces in which the knotoid can be immersed without any virtual crossings. Virtual knotoids that can be represented by a classical knotoid diagram are called *genus 0-knotoids*. At the time of writing this paper we do not know if the theory of classical knotoids embeds into the theory of virtual knotoids. We conjecture the following.

Conjecture 3.5. *Two virtually equivalent classical knotoid diagrams are equivalent using only classical $\Omega_{i=1,2,3}$ - moves.*

Note that any virtual knotoid invariant is also an invariant for classical knotoids since the generalized Ω - moves include $\Omega_{i=1,2,3}$ - moves.

Remark 1. The definitions we have used so far and Theorem 3.2 directly generalizes to virtual multi-knotoid diagrams. A *virtual multi-knotoid diagram* is an immersion of finitely many oriented circles and the oriented unit interval into S^2 with finitely many transversal double points that correspond to classical and virtual crossings. And the virtual equivalence defined for virtual knotoids generalizes to virtual multi-knotoids in the obvious way.

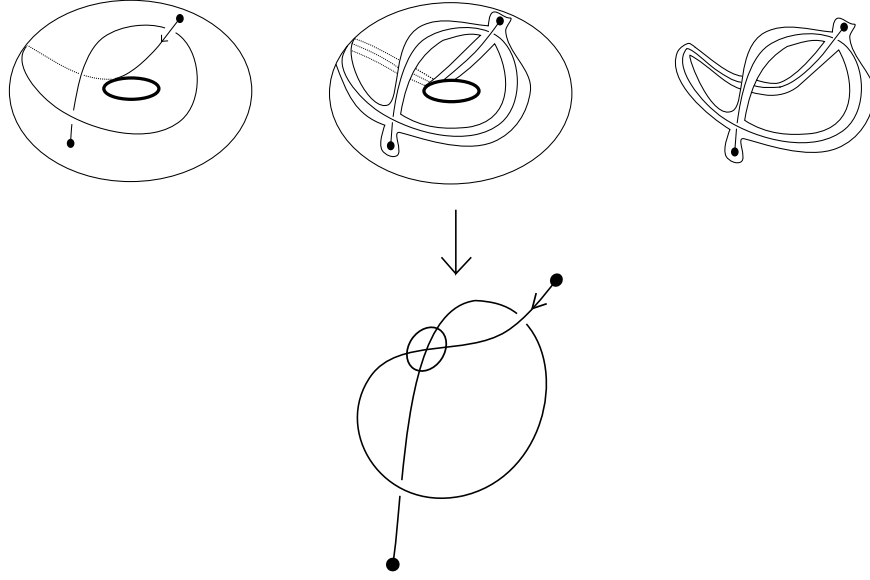


FIGURE 11. Virtual knotoid and abstract knotoid diagram

3.2. Flat Knotoids. A *flat virtual knotoid diagram* is a knotoid diagram in S^2 with virtual crossings and *flat crossings* that are obtained by omitting the under/over-crossing information of the classical crossings. *Flat $\Omega_{i=1,2,3}$ - moves* ignore the under/over-crossing information of the crossings in the corresponding move patterns Ω_1 , Ω_2 and Ω_3 , respectively. The moves on flat knotoid diagrams generated by the flat $\Omega_{i=1,2,3}$ and the detour move, are called *generalized flat Ω - moves*.

Two flat virtual knotoid diagrams are said to be *f-equivalent* if there is a finite sequence of flat generalized Ω - moves and isotopies of S^2 taking one another. Two flat classical knotoid diagrams are said to be *f-equivalent* if there is a finite sequence of flat $\Omega_{i=1,2,3}$ - moves and isotopies of S^2 taking one diagram to the other. A *flat classical knotoid* is considered an equivalence class of all f-equivalent classical knotoid diagrams.

It is well-known that any flat classical knot is equivalent to the unknot (by taking an ascending diagram that overlies the flat classical knot diagram and applying an unknotting sequence to the overlying diagram, one obtains an unknotting sequence for the flat diagram). This property of flat classical knots generalizes to flat classical knotoids.

Proposition 3.6. *Any flat classical knotoid is f -equivalent to the trivial knotoid.*

Proof. Any flat classical knotoid diagram is f -equivalent to a flat knotoid diagram with any one of its endpoints lying in the unbounded region of the 2-sphere. This equivalence can be obtained by an isotopy of $S^2 = \mathbb{R}^2 \cup \infty$: We pull the strands that lie between the chosen endpoint (let it be the tail) and the ∞ -point towards the ∞ -point and then across the ∞ -point all along S^2 to bring the strands back to the diagram and leave the endpoint in the unbounded region of S^2 . Without loss of generality, we take into consideration flat knotoid diagrams with the tail lying in the unbounded region. A classical knotoid diagram is essentially formed by loops each associated with the crossings of the diagram. We say the *loop at c* for the loop formed by a crossing c . In flat knotoid diagrams, loops are formed by flat crossings. There are two types of loops in a flat classical knotoid diagram: A loop which does not surround the other endpoint, the head, but intersects with other loops transversely along finitely many strands that go through the inside of the loop and the other type of loops surrounds the head and also intersects with other loops transversely. Figure 12 is an illustration for loops of the two types.

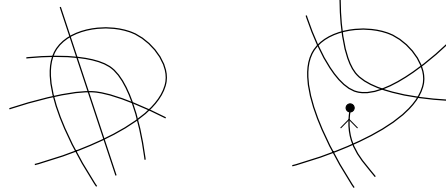
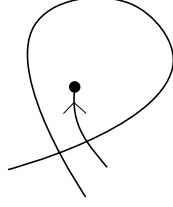


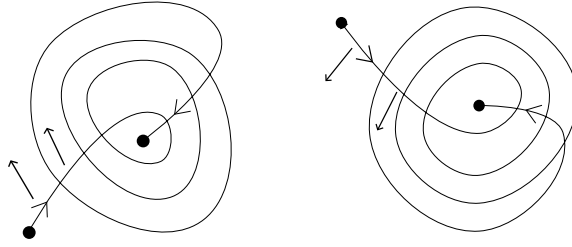
FIGURE 12. Two types of loops at classical crossings

Let K be a flat knotoid diagram representing a flat classical knotoid. Let α be a loop of the first type at a crossing of K . Transversal strands that pass through the inside of α intersecting the loop at two points, can be taken out of α by finitely many flat Ω_2 - and Ω_3 -moves. After eliminating all strands within the region, the Ω_1 -move is available to undo the loop α , meaning that we reduce the number of the loops in the diagram by 1. Loops of the first type are eliminated one by one in the same way. If all loops of K are of the first type, that is, if the diagram is a knot-type knotoid diagram then the diagram reduces to the trivial knotoid diagram immediately.

If there are remaining loops of the second type, enumerate them with respect to the order of the formation. Start pulling the transversal strands out of the first loop: Each transversal strand which intersects the loop at two distinct points, divides the region bounded by the loop into two closed sub-regions. One of the regions does not contain the head by the Jordan curve theorem, so flat Ω_3 - and Ω_2 -moves are available in that region for taking the strands out of the loop (it is forbidden to pull a strand across the head so the moves are not available in the other sub-region). Apply the available Ω_3 and Ω_2 -moves to turn the loop in to an *innermost loop*: a loop penetrated by only the strand of head of the diagram, as illustrated in the Figure 13.

FIGURE 13. **An innermost loop**

It is possible that some of the enumerated loops of the second type become a loop of the first type so they can be undone as explained above. The remaining enumerated loops contain both the head and transversely intersecting strands also includes the innermost loop obtained from the first loop. Choose the next loop and start pulling the strands out of the loop. We do this again by the available Ω_2 - and Ω_3 - moves along the sub-regions of the loop where the head is not located. Thus this loop becomes an innermost loop. The same procedure applies the rest of the loops and a spiral knotoid diagram of K is obtained.

FIGURE 14. **Two types of spiral knotoid diagrams**

In a *spiral knotoid diagram*, the tail is in the unbounded region of S^2 and all loops at crossings contain the head and they do not intersect with other loops transversely. We have two types of spiral knotoid diagrams due to the orientation. We depict an example of flat spiral knotoid diagrams of each type in Figure 14.

Any spiral flat classical knotoid diagram can be undone. Pick up the tail and start sliding the strand adjacent to the tail in depending on the orientation type of the spiral. Whenever we meet with a crossing, pass the strand across the crossing with a flat Ω_3 -move and then apply a flat Ω_2 that reduces the crossing number and sets the strand free of the former crossing. At each crossing the same will apply. Continue to slide the strand using this procedure at each crossing that is met until the spiral is undone and thus we have the trivial knotoid diagram. Thus K can be turned into the trivial knotoid diagram. \square

An *ascending* knotoid diagram consists of crossings which are met first as over-crossings during a trip from the tail to the head. Similar to flat classical knotoid diagrams, any ascending classical knotoid diagram can be turned into a diagram with the tail lying in the unbounded region of S^2 . We work with such diagrams with tails in the unbounded region. Ascending knotoid diagrams are formed by two types of loops associated to the crossings of the diagram. The difference from the loops of a flat knotoid diagram is that the strands

intersecting transversally with a loop enter/leave the loop either as an undercrossing or an overcrossing.

If a strand enters into the loop as an overcrossing (respectively undercrossing) then it leaves the loop as an overcrossing (respectively undercrossing). This is caused by definition: For a strand entering the loop as an overcrossing means that the strand is traversed prior to the loop during the trip along the diagram (from the tail to the head). This makes Ω_2 - and Ω_3 - moves available for cleaning the loops from transversal strands and provides an ascending spiral knotoid diagram. Any ascending spiral diagram can be undone by sliding the strand next to the tail in the direction of orientation, and by using available Ω_2 - and Ω_3 - moves to save the strand from the crossings met with. Therefore we have the following corollary.

Corollary 3.1. *Any ascending classical knotoid diagram is equivalent to the trivial knotoid diagram.*

Note that unlike the classical case, there are flat virtual knotoids which are non-trivial. In section 4.2 we discuss an example for this with the discussion of the parity bracket polynomial.

We say that a virtual knotoid diagram *overlies* a flat diagram if it is obtained from the flat diagram by choosing a crossing type as over or under for each flat crossing. In fact, every virtual knotoid diagram K overlies a flat virtual knotoid diagram $F(K)$ that is obtained by omitting the extra information at classical crossings of K . If K and \widehat{K} are virtually equivalent virtual knotoid diagrams then $F(K)$ and $F(\widehat{K})$ are flat-equivalent since generalized Ω -moves induce flat generalized Ω -moves on the associated flat diagrams. Thus a virtual knotoid diagram is necessarily nontrivial if the associated flat diagram is not trivial.

3.3. The Virtual Closure of Knotoids. Two ways to represent a classical knot via the classical knotoids were explained in Section 2. Every classical knotoid represents a virtual knot as well, as pointed out by O. Viro [34]. An embedded arc in S^2 that is connecting the endpoints of a given classical knotoid diagram, is chosen to create a virtual crossing whenever it meets with a strand of the diagram.

Definition 5. The connection operation indicated above and depicted in Figure 15, is called *virtual closure* of classical knotoids, and defines a well-defined map denoted by \bar{v} ,

$$\bar{v}: \text{Classical Knotoids} \rightarrow \text{Virtual Knots of genus } \leq 1$$

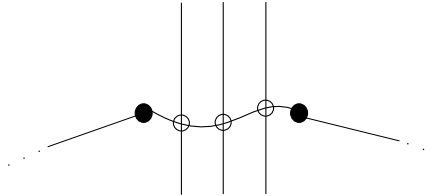


FIGURE 15. The virtual closure of a knotoid diagram

It is not hard to see that \bar{v} respects the equivalence classes of classical knotoids. Any choice of the connection arc does not alter the isotopy class of the virtual knot that is obtained,

in fact, the isotopy between any two shortcuts transform to a detour move between the corresponding virtual knot diagrams. Knot-type knotoid diagrams close virtually to classical knots. The underpass closure and the virtual closure of knot type knotoids give equivalent classical knots. The virtual closure of a proper knotoid diagram is a virtual knot diagram with the virtual crossings are positioned consecutively over the connection arc. By attaching a 1-handle to the sphere of this diagram that holds the connection arc containing the virtual crossings, the knot diagram is represented in a torus. Thus, the virtual closure of a classical knotoid can be at most a genus one virtual knot.

The virtual closure map is not injective. Figure 19 shows an example of a pair of nonequivalent knotoid diagrams both close to the same virtual knot. The non-equivalency of these diagrams can be detected by the bracket polynomial of knotoids. The bracket polynomial of knotoids in S^2 was defined by V. Turaev [34], by extending the the state expansion of the bracket polynomial of knots [16,18] for knotoids. There are two ways of smoothing a classical crossing of a knotoid diagram K , by *A-smoothing* or in *B-smoothing*. A *state* of a knotoid diagram K is a choice of smoothing for each classical crossing with labels. A state is labeled by 1 if A-smoothing is applied and labeled by -1 if B-smoothing is applied at a particular crossing. Smoothing all crossings of a knotoid diagram results in embedded circular components and a single long segment component with two endpoints. See Figure 16 for the state expansion of the bracket polynomial.

The bracket polynomial for K is defined as

$$\langle K \rangle = \sum_S A^{\sigma(S)} d^{\|S\|-1}$$

where the sum is taken over all states, $\sigma(S)$ is the sum of the labels of the state S and $\|S\|$ is the number of components of S and $d = (-A^2 - A^{-2})$.

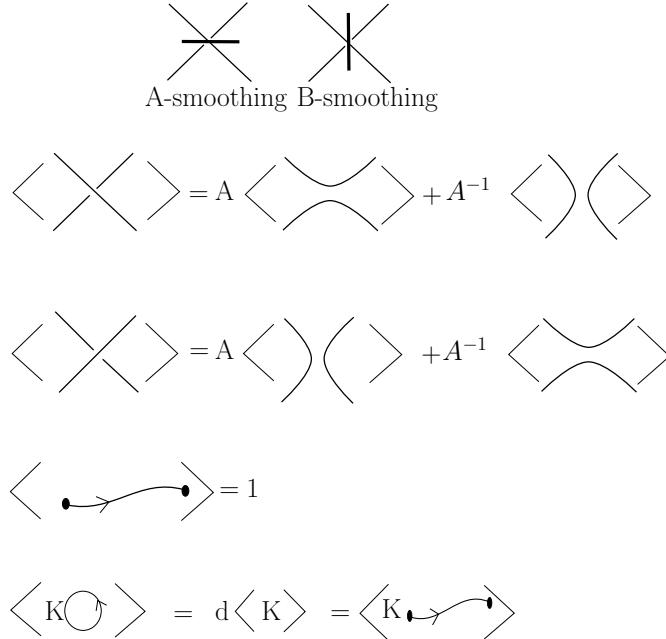


FIGURE 16. Skein relations of the bracket polynomial

The bracket polynomial turns into an invariant for both classical and virtual knotoids with a normalization by the writhe. The *writhe* of a knotoid diagram K , $wr(K)$ is the number of positive crossings (the crossings with sign $+1$) minus the number of negative crossings (the crossings with sign -1) of K . The writhe is invariant under the generalized Ω -moves except that Ω_1 -move changes the writhe by ± 1 .

The normalized bracket polynomial is defined as,

$$f_K = (-A^3)^{-wr(K)} \langle K \rangle$$

and it extends the Jones polynomial to classical knotoids with a substitution $A = t^{-1/4}$.

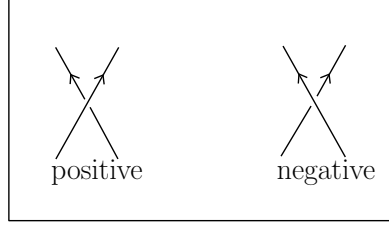


FIGURE 17. Crossing types

Example 3.1. Let K_1 and K_2 be the knotoid diagrams given in Figure 19, respectively. We compute that $\langle K_1 \rangle = A^2 + 1 - A^{-4}$ and $\langle K_2 \rangle = 1 - A^4 + A^{-2}$. The computation of the bracket polynomial of K_1 is shown in Figure 18. These classical knotoid diagrams are not equivalent since their normalized bracket polynomials are different. As we can also see from the picture, the virtual closures of them are the same virtual knot. Therefore, the virtual closure map is not injective.

$$\begin{aligned}
 \langle \text{Diagram 1} \rangle &= A \langle \text{Diagram 2} \rangle + A^{-1} \langle \text{Diagram 3} \rangle \\
 &= A(A \langle \text{Diagram 4} \rangle + A^{-1} \langle \text{Diagram 5} \rangle) + A^{-4} \langle \text{Diagram 6} \rangle \\
 &= (A^2 + 1 - A^{-4}) \langle \text{Diagram 7} \rangle
 \end{aligned}$$

FIGURE 18. Computation of the bracket polynomial of K_1

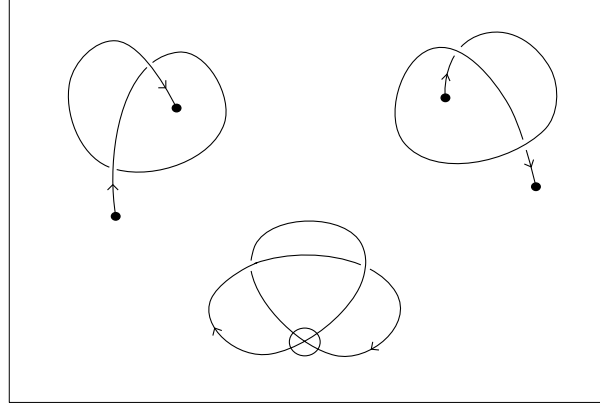


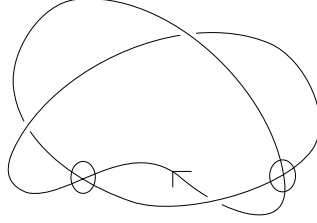
FIGURE 19. **Nonequivalent classical knotoids with the same virtual closure**

The well-known Jones polynomial conjecture can be extended to a conjecture for classical knotoids.

Conjecture 3.7. *The normalized bracket polynomial (or Jones polynomial) detects the trivial knotoid.*

This generalization of the knot detection conjecture for the classical Jones polynomial may have an analogue in Khovanov homology for knotoids. We shall explore this question in a sequel to the present paper. The reader should note that Khovanov homology detects the unknot [19].

If a virtual knot is represented by a diagram with virtual crossings which are consecutively positioned on the same strand, then it is immediate to conclude that this virtual knot is in the image of the virtual closure map. In particular, the knots 2.1,3.2, 4.12, 4.43, 4.65, 4.94, 4.100 listed in [9] are genus 1 virtual knots which are the virtual closures of some classical knotoids. For a virtual knot given by a diagram with arbitrarily positioned virtual crossings, we want to know whether this virtual knot is in the image of the virtual closure map. The virtual knot k which is given in Figure 20 and listed as virtual knot 3.1 in [9], is a nontrivial genus one virtual knot with trivial Jones polynomial. We conjecture that the virtual knot k is not in the image of the virtual closure map which shows this map is not surjective. If the given knot were in the image then we would have a classical knotoid K that is nontrivial but has unit Jones polynomial since the Jones polynomial of K is equal to the Jones polynomial of k . Hence our conjecture about the Jones polynomial implies that k is not in the image and therefore the virtual closure map is not surjective.

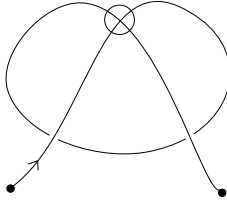
FIGURE 20. **The virtual knot 3.1**

Being a well-defined map, the virtual closure map sets a way to construct many invariants for classical knotoids which generalize to a virtual knotoid invariant. In fact, if $\text{Inv}(K)$ denotes any invariant of virtual knots then we can define a knotoid invariant $\text{Inv}(K)$ for any classical knotoid K by the following formula,

$$\text{Inv}(K) = \text{Inv}(\bar{v}(K))$$

This formula is our main motivation for constructing the invariants of this paper.

The virtual closure map can be extended to a well-defined map from the set of virtual knotoids to the set of virtual knots. We call this map *extended virtual closure map*. It is obvious that the extended virtual closure map is a surjective map. But the map is still not injective. Any virtual knotoid diagram with endpoints located in the same region can be regarded as a long virtual diagram. The virtual knotoid in Figure 21 is known to be a nontrivial long virtual knot [13]. The virtual closure of this knotoid is the trivial knot thus it is a nontrivial element of the kernel of the extended virtual closure map. The non-triviality of this knotoid can be detected by the parity bracket polynomial of knotoids that will be discussed in Section 4.2.

FIGURE 21. **A nontrivial virtual knotoid with trivial virtual closure**

The kernel of the virtual closure map is an interesting task to be explored. If we restrict the virtual closure map to knot-type knotoids then the kernel is trivial. In fact, if a knot type knotoid is nontrivial then the virtual closure is a nontrivial virtual knot since the knot in the closure is topologically the same as the knotoid. But, *does there exist a proper knotoid whose virtual closure is the trivial knot?* If our conjecture on Jones polynomial holds then we can answer this question. Note that the Jones polynomial of a classical knotoid is the same as the Jones polynomial of the virtual knot obtained by the virtual closure. Therefore, our conjecture implies that there does not exist any proper knotoid whose virtual closure is the trivial knot.

Remark 2. The underpass closure can not be extended to virtual knotoid diagrams in a well-defined way. Figure 22 depicts a virtual knotoid diagram that represents two virtual

knots via the underpass closure. To transform one diagram to the other one we require the virtual forbidden move, Φ_{under} which is shown in Figure 8. The arrow polynomial which will be discussed in Section 5, detects that these knots are not equivalent.

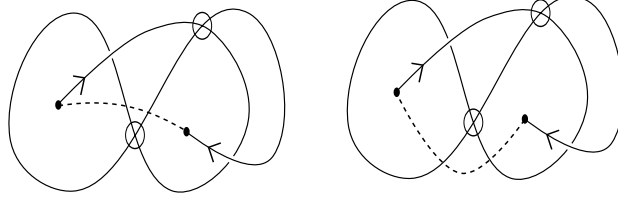


FIGURE 22. A virtual knotoid diagram representing different knots via ω_-

4. PARITY AND ODD WRITHE

4.1. Gauss Code. The *Gauss code* of a knotoid diagram K is a linear code which consists of a sequence of labels corresponding to the classical crossings encountered during a trip along the diagram from tail to the head. Each label in the code is repeated twice in the code since every crossing is traversed twice, so the length of the code is $2n$ for n is the number of classical crossings of K . We keep the information of the passage through a crossing either as an overcrossing or an undercrossing by adding the symbols O and U to the code and we keep the signs of the crossings by putting $+$ or $-$ next to the label accordingly to the sign of the crossing. The resulting code is referred as the *signed Gauss code* of K . The symbols O and U and the signs of crossings are omitted in the Gauss codes of flat diagrams.

Gauss codes have a diagrammatic representation as follows. Each label in the Gauss code of a knotoid diagram is represented by $2n$ labeled points placed upon a segment which is oriented from left to right. A signed and oriented chord connects each pair of the labeled points. The orientation of a chord heads from the overcrossing to the undercrossing. That is, during our travel along the knotoid diagram starting from the tail, if a crossing is first encountered as an overcrossing then the arrow of the corresponding chord heads towards the second appearance of the label. The sign of the chord is the sign of the associated crossing. For flat knotoid diagrams, we have the notion of right and left at each classical crossing. If a crossing is first encountered as going to the right then the head of the arrow on the corresponding chord heads towards the first appearance of the label. Figure 23 depicts the chord diagram of the knotoid diagram in Figure 1g. This way we have *Chord diagrams* that represent Gauss codes of knotoids in a unique way. To every knotoid diagram, there is a uniquely associated chord diagram.

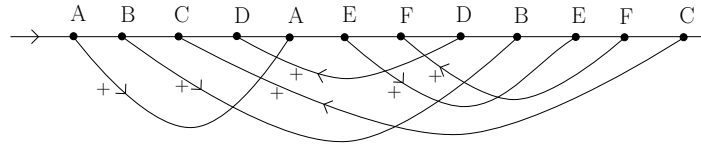


FIGURE 23. Chord diagram of the knotoid diagram in Figure 1g

The Gauss code of the knotoid diagram whose chord diagram is given above is

$$OA + OB + UC + UD + UA + OE + UF + OD + UB + UE + OF + OC +$$

and

$$ABCD AEFDBEFC$$

is the Gauss code of the associated flat knotoid diagram. For the purpose of parity we may use the flat Gauss code.

Definition 6. A single component Gauss code is said to be *evenly intersticed* if there is an even number of labels between two appearances of any label.

Any classical knot diagram has evenly intersticed Gauss code [31]. The important fact is that the Gauss codes of classical knotoid diagrams are not necessarily evenly intersticed. This fact gives rise to a well-defined parity for the crossings of classical knotoid diagrams: Each crossing is regarded as either *even* or *odd*. A crossing of a classical or virtual knotoid diagram is called *odd* if there is an odd number of labels in between the two appearances of the crossing otherwise it is called an *even* crossing. In Figure 23 we see that the chord diagram of the classical diagram shown in Figure 1g that is not evenly intersticed and the crossings A, D, E and F are odd and the crossings B, C are even.

Theorem 4.1. *The Gauss code of a classical knotoid diagram is evenly intersticed if and only if it is a knot-type knotoid diagram, that is, the tail and the head of the diagram lie in the same local region of S^2 .*

Proof. Let K be a proper knotoid diagram. Each crossing of K forms a loop. Then one of the endpoints of K is separated from the other one by at least one loop which is associated to a crossing, that is, one of the endpoints is located inside at least one loop at a crossing. All the strands entering the loop except the one that is adjacent to the endpoint, leave the loop by Jordan curve theorem. Thus each such strand contributes with a pair of labels to the Gauss code of the diagram. The Gauss code along this loop is in the following pattern: $\dots c \dots d a e \dots \bar{a} \dots \bar{e} c \dots$, where c represents the crossing that forms the loop containing the endpoint, d represents the crossing of the strand adjacent to the endpoint with the loop, and a, \bar{a} and e, \bar{e} for the pairs of crossings created by the transversely intersecting strands which enter and leave the loop. Thus, between the two appearances of the label c , we have an odd number of labels so that the Gauss code of K is not evenly-intersticed. For K a knot-type diagram, we can assume that the tail and head lie in the unbounded region of S^2 so that none of the loops at crossings contain them. Again by Jordan curve theorem, all the strands passing through any of the loops of K enter and leave the loop so that they contribute with a pair of labels to the Gauss code of K . This shows that each crossing is even, that is, the Gauss code of K is evenly-intersticed. \square

Lemma 4.2. *The Gauss code of a knotoid diagram, either classical or virtual, is the same as the Gauss code of its virtual closure.*

Proof. The virtual closure map creates only virtual crossings to a given diagram so it does not have an effect on the Gauss code of the diagram. \square

Definition 7. Using the parity of crossings, we define the *odd writhe* for both classical and virtual knotoid diagrams as the sum of the signs of the odd crossings:

$$\text{Odd Writhe of } K = J(K) = \sum_{c \in \text{Odd}(K)} \text{sign}(c)$$

where K is a knotoid diagram and $\text{Odd}(K)$ is the set of odd crossings in K .

Theorem 4.3. *Odd writhe is a virtual knotoid invariant.*

Proof. The odd writhe is invariant under the virtual moves; including the virtual $\Omega_{i=1,2,3}$, the partial virtual move and the Ω_v - move since these moves do not have any effect on the structure of Gauss code so on the set of odd crossings, by definition. Thus it suffices to verify the invariance under the classical $\Omega_{i=1,2,3}$ -moves.

The Ω_1 -move adds/removes two consecutive labels in the Gauss code. Thus the parity of crossings remain the same and being an even crossing the added/removed crossing does not affect the odd writhe.

The Ω_2 -move adds/removes either a pair of even crossings or a pair of odd crossings with opposite signs for any orientation type of the move. In the former case the even crossings do not have any effect on the odd writhe. In the latter case, the two odd crossings will be canceled out in the odd writhe summation for they have opposite signs. The parity of the crossings located outside the Ω_2 move region, remains the same since the labels which are added/removed by one Ω_2 -move are located as consecutive pairs in the the Gauss code.

Figure 24 depicts corresponding Gauss codes of the diagrams related to each other by one Ω_3 - move. One can see that the triangular move pattern of Ω_3 -move can contain either three even crossings or two odd crossings and one even crossing. In the former case, these even crossings are taken to even crossings by Ω_3 -move and the parity of other crossings outside the move pattern remains the same thus the odd writhe is not affected. In the latter case, Ω_3 - move only permutes the two odd crossings in the Gauss code and the parity and the signs of the odd crossings remain the same. It is again not hard to see that the parity of crossings outside the move pattern does not change. Therefore the odd writhe is invariant under the $\Omega_{i=1,2,3}$ - moves. \square

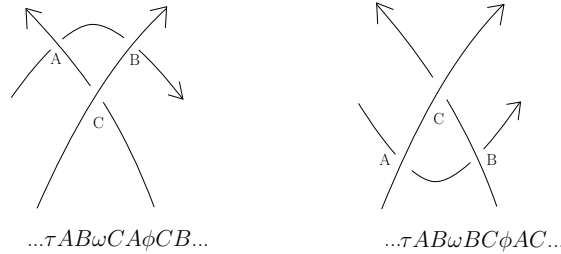


FIGURE 24. Gauss code under one Ω_3 - move

Corollary 4.1. If a knotoid K is of knot-type then the odd writhe of K is zero.

Proof. It follows from Theorem 4.1 and from the invariance of the odd writhe, that $J(K) = 0$. \square

Note that Theorem 4.1 does not hold for virtual knotoid diagrams. For instance, in Figure 21 we have a virtual knotoid diagram with its endpoints located in the same region. The Gauss code of this knotoid diagram is $O1 + U2 - U1 + O2-$ that is not evenly intersticed.

Remark 3. The parity defined for knotoids does not extend directly to a parity for multi-knotoids. The crossings shared by any two components of a multi-knotoid diagram present an obstacle for extending this parity. The following figure depicts an example for the obstruction.

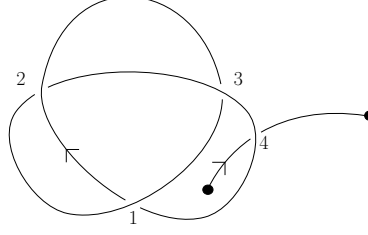


FIGURE 25. A multi-knotoid diagram

The Gauss code of the multi-knotoid in Figure 25 is $O1 - U2 - O3 - O4 + U1 - O2 - U3 - /U4+$. Crossings 1, 2 and 3 are even crossings in the circular component but the crossings are odd if the second component is considered. To define a well-defined parity for multi-knotoids, we use the idea of V. Manturov for extending the parity to virtual links [10, 11, 24]. We regard the crossings of a multi-knotoid diagram that are shared by two components as *link crossings*. So the parity remains the same for self-crossings of each component, as odd or even and we add a new type of crossing, a link crossing. Therefore, in the diagram given in Figure 25, the crossings 1, 2, 3 are even and 4 is a link crossing.

4.2. Parity Bracket Polynomial. The parity bracket polynomial of V. Manturov [24] is a modification of the bracket polynomial that uses the parity of crossings in virtual knots and links. With the existence of even and odd crossings in knotoid diagrams, the parity bracket polynomial can be defined for both classical knotoids and virtual knotoids. For K is a knotoid diagram either classical or virtual, a *parity state* is defined to be a labeled graph (a virtual graph for virtual diagrams). A parity state is obtained by smoothing the even crossings by A- and B- smoothing of the usual bracket polynomial and labeling the smoothing sites by A or A^{-1} , and the odd crossings of K are replaced by graphical nodes.

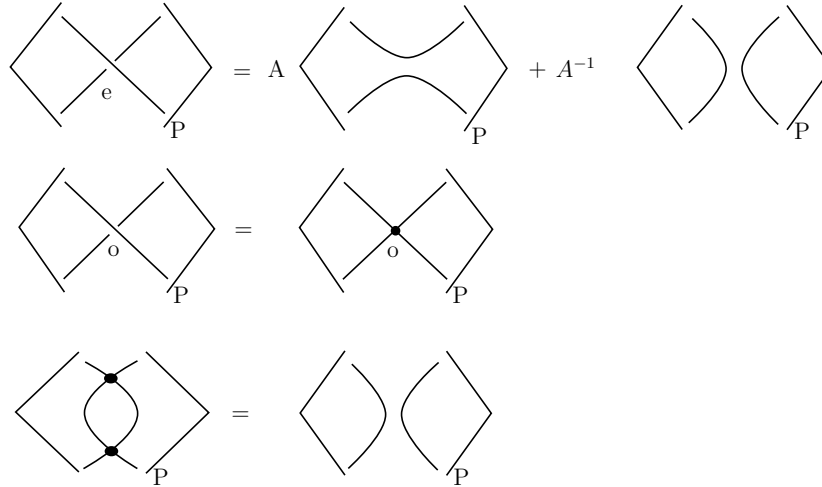


FIGURE 26. Parity bracket expansion

The resulting virtual graphs are taken up to the virtual equivalence (isotopy of S^2 and detour moves) and up to the *reduction rule*, shown in Figure 26. The reduction rule is simply a Reidemeister two- move reducing the number of nodes in a graphical state. The graphical

states which still contain nodes are *irreducible* states and contribute to the polynomial as graphical coefficients. The parity bracket of K is defined as

$$\langle K \rangle_P = \sum_S A^{n(S)} (-A^2 - A^{-2})^{l(S)} G(S)$$

where $n(S)$ denotes the number of A -smoothings minus B -smoothings, $l(S)$ is the number of standard components (without any nodes) in the state S and $G(S)$ is the union of reduced graphical states containing graphical nodes.

The Ω_1 -move adds/removes an even crossing and changes the polynomial by $-A^{\pm 3}$. We normalize the polynomial by the writhe to obtain a virtual knotoid invariant.

Definition 8. *The normalized parity bracket polynomial of a knotoid diagram K is defined as*

$$P_K = (-A^3)^{-\text{wr}(K)} \langle K \rangle_P.$$

Theorem 4.4. *The normalized parity bracket polynomial is a virtual knotoid invariant.*

Proof. It suffices to check the local changes by $\Omega_{i=1,2,3}$ - moves. The writhe normalization makes the parity polynomial invariant under Ω_1 - move. The invariance under Ω_2 - move follows from the bracket polynomial invariance if the two crossings in this move pattern are both even crossings. If they are odd crossings instead, the reduction rule applies to these crossings and the polynomial does not change by Ω_2 - move. The invariance under Ω_3 - move, if three of the crossings in the triangular region are even, follows from the bracket polynomial invariance, and if two of them are odd and one is an even crossing then the invariance follows by an isotopy of the state component. \square

Theorem 4.5. *The normalized parity bracket polynomial is an invariant of flat virtual knotoids if $A = -1$ and $\delta = -2$. The normalized parity bracket polynomial of any classical knotoid is trivial.*

Proof. The invariance can be seen easily by the check of the invariance under the flat $\Omega_{i=1,2,3}$ - moves. Since any flat classical knotoid is f-equivalent to the trivial knotoid, the second statement follows. \square

Knot-type knotoid diagrams contain no odd crossings so there is no graphical coefficient contributing to the parity bracket polynomial of knot-type knotoids. In fact, the parity bracket polynomial of knot-type knotoids coincides with the usual bracket polynomial of knotoids. Proper knotoid diagrams have odd crossings so we observe graphical states in the parity expansion. But the reduction rule eliminates all the graphical states. In fact, we have the following proposition.

Proposition 4.6. *There are no irreducible state components in the parity state expansion of classical knotoid diagrams.*

Proof. Let K be a classical knotoid diagram. Graphical states include only the nodes representing the odd crossings of K . The set of odd crossings of K is the same with the set of odd crossings of $F(K)$ where $F(K)$ is the associated flat diagram which is a flat classical diagram. For this reason, the existence of an irreducible graphical state in parity states of K would cause an irreducible graphical state in the parity states of $F(K)$. Thus it is sufficient to show that any graphical state component of a flat classical knotoid can reduce to a component which is free of nodes. Proposition 3.6 implies that a flat classical knotoid diagram

can be obtained from the trivial knotoid diagram by finitely many flat $\Omega_{i=1,2,3}$ -moves. We induct on the number of $\Omega_{i=1,2,3}$ - moves applied to the trivial knotoid diagram.

The trivial knotoid diagram has trivial parity bracket polynomial so it satisfies the claim. We assume that all flat diagrams which are $n > 0$ flat Ω_i - moves away from the trivial diagram, that is, flat diagrams which are obtained from the trivial diagram by n flat Ω_i -moves, satisfy the claim. A single flat Ω_2 -move may add two odd crossings to an n -away flat diagram but they do not change the parity of the other crossings as mentioned in the proof of Theorem 4.4. These two odd crossings appear as the nodes of a bigon and can be eliminated by the reduction rule. So we fall back to the former case for which all graphical states are reducible. The flat Ω_3 - move does not add/remove any odd or even crossings, so the graphical state of the former diagram which is assumed to be reducible is just carried to an isotopic graphical state which is also reducible. The flat Ω_1 -move adds/removes an even crossing which does not change the parity of the crossings and does not add any nodes to the diagram, so the graphical states are not affected. This proves the induction hypothesis: The parity states of a flat classical knotoid diagram reduce to states that are free of nodes. Therefore the parity states of classical knotoid diagrams are all reducible. \square

Lemma 4.7. *For \tilde{K} a classical knotoid we have $\langle \tilde{K} \rangle_P = \langle \bar{v}(\tilde{K}) \rangle_P$.*

Proof. We have just shown that graphical state components of a classical knotoid diagram are reducible so that the states consist of embedded circular components and one single long segment component. Let K be a classical knotoid diagram representing \tilde{K} . The contribution of each state component of K to the polynomial is the same as the contribution of the components which are the virtual closures of the long segment component of each state. The skein relations of the parity bracket do not smooth or remove the virtual crossings added to the knotoid diagram during the virtual closure. If any of these virtual crossings lies inside any of the bigon-region of reduction for a state of the closure knot then we can take the crossings out of the region by the detour move, so the graphical states obtained are reducible just as the graphical states of the knotoid are reducible. Connecting the endpoints of the segment components virtually gives the parity states of the virtual knot, $\bar{v}(K)$. Therefore, $\langle K \rangle_P = \langle \bar{v}(K) \rangle_P$. \square

Corollary 4.2. *If there are graphical coefficients in the parity bracket of a virtual knot K then K is not the virtual closure of a classical knotoid.*

Proof. It follows by Proposition 4.6 and Lemma 4.7. \square

The graphical states of a virtual knotoid are not necessarily reducible. A closer look at reducible graphical states is helpful for determining the reducibility of a given state. We label each edge of the state. The nodes that share exactly two edges (e and b) form a reducible configuration iff one node has order $e b f c$ and the other $b e a d$ in the counterclockwise orders. Then up to detour moves, a virtual knotoid diagram will have a removable bigon between the nodes, as shown in Figure 27.

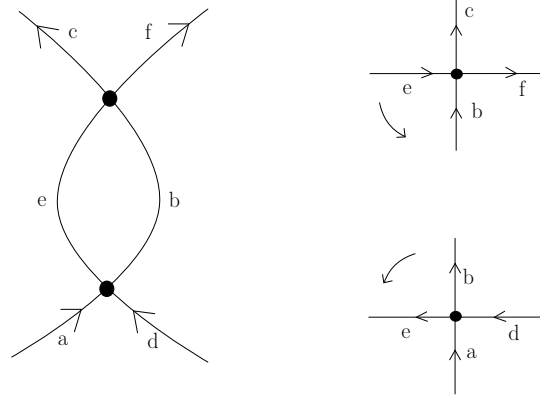
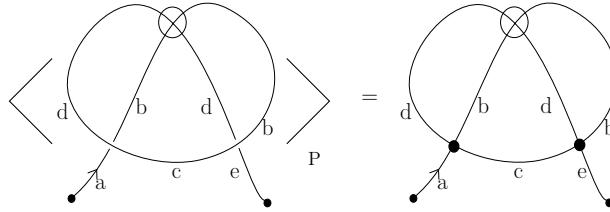


FIGURE 27. Labels at the nodes of a reducible bigon

Two of the classical crossings of the virtual knotoid diagram given in Figure 21 are odd crossings. There is only one parity state of this diagram that is a graphical state, obtained by replacing these crossings by nodes. The two nodes have orders: $a c b d$ and $e b d c$, respectively. Since the shared edges b and d do not appear in the required order, the state is not reducible. We conclude that the parity bracket polynomial consists of one summand that is a graphical coefficient, see Figure 28. Thus the non-triviality of this virtual knotoid whose virtual closure is trivial, is justified with the parity bracket polynomial. By Proposition 4.6, this virtual knotoid diagram is not virtually equivalent to a classical knotoid diagram, and in fact, it represents a genus one virtual knotoid.

FIGURE 28. 1st node: $acbd$ 2nd node: $ebdc$

The necessary condition given above for eliminating the nodes of a graphical state applies in the same way to the flat case. The parity bracket polynomial of the associated flat diagram to Figure 21 is the same as the polynomial of the overlying virtual knotoid, consisting of one graphical coefficient. Therefore, the parity bracket polynomial of this flat virtual knotoid diagram is not trivial. This completes the argument in Section 3.2 that flat virtual knotoids are not necessarily trivial.

Remark 4. The normalized parity bracket polynomial extends to an invariant for virtual multi-knotoids. *Even* crossings of a multi-knotoid diagram are smoothed in the usual way. Together with the *odd* crossings, *link crossings* (crossings between distinct components) of a multi-knotoid diagram are replaced by graphical nodes. We extend the procedure for calculation of the parity bracket polynomial to include the link crossings: we reduce the graphical states containing the nodes corresponding to link crossings, by the same reduction

rule. Irreducible graphical states contribute to the polynomial as graphical coefficients. The parity bracket polynomial of a virtual multi-knotoid is defined in the same way by expanding the state summation, and the normalization of the polynomial with writhe is a virtual multi-knotoid invariant.

We have showed that the graphical components of a classical knotoid are all reduced by the reduction rule and they are free of nodes. Unlike this, a classical multi-knotoid may have irreducible graphical states. The simplest nontrivial multi-knotoid with two components, given in Figure 29 consists of one link crossing. Then it has a nontrivial parity bracket polynomial which is equal to one graphical coefficient.

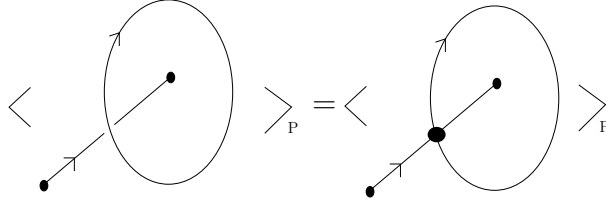


FIGURE 29. A multi-knotoid with nontrivial parity bracket

4.3. Affine Index Polynomial. The affine index polynomial was defined first for virtual knots and links by L.H. Kauffman [17]. It is a one variable Laurent polynomial taking values in the ring $\mathbb{Z}[t, t^{-1}]$ whose construction depends on an integer labeling assigned to flat virtual knot diagrams in the following way.

An *arc* of an oriented flat virtual knot diagram is an edge which extends from one classical vertex to the next vertex. Each arc can be labeled by an integer as follows. We start from an arbitrary point of the diagram and label the arc that the point lies upon with an integer a , and then if the labeled arc meets with a classical vertex and if it crosses towards left then the arc changes into a new arc with a label increased by one, $a + 1$, if the arc crosses towards right then the next arc is labeled by $a - 1$. There is no change of labels at a virtual crossing.

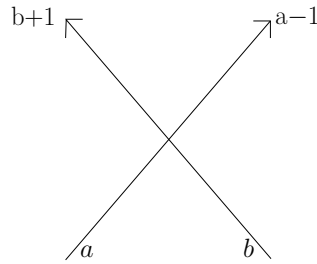


FIGURE 30. Integer labeling at a flat crossing

Definition 9. Let K be a virtual knot diagram and $F(K)$ is the associated flat diagram. There are two number outcomes at each labeled flat crossing of $F(K)$. For c is a classical crossing of K the two numbers, $w_+(c)$ and $w_-(c)$ are called *positive* and *negative* weights of

c , respectively. The $w_+(c)$ and $w_-(c)$ are defined as

$$\begin{aligned} w_+(c) &= a - (b + 1) \\ w_-(c) &= b - (a - 1). \end{aligned}$$

where a and b are the labels for the left and the right incoming arcs at the corresponding flat crossing to c , respectively (see Figure 30).

The *weight* of c is then defined as

$$w_K(c) = \begin{cases} w_+(c) & \text{if the sign of } c \text{ is a positive,} \\ w_-(c) & \text{if the sign of } c \text{ is a negative} \end{cases}$$

The *affine index polynomial* of a virtual knot K is defined by the equation:

$$P_K(t) = \sum_c \text{sgn}(c)(t^{w_K(c)} - 1)$$

where the sum is taken over all classical crossings of a diagram of K and $\text{sgn}(c)$ is the sign of c .

Both classical and virtual flat knotoid diagrams admit such an integer labeling. An *arc* of a flat knotoid diagram extends from one flat crossing to the next one and also connects the tail and the head to the first and the last crossing, respectively. Given a knotoid diagram K , we begin labeling the arc adjacent to the tail of the associated flat diagram and change labels at each flat crossing with the same rule as explained above. Therefore we can define the *affine index polynomial* for knotoid diagrams exactly as defined for virtual knots by using the weights of classical crossings just described.

The numbers at c , $w_+(c)$ and $w_-(c)$ are defined as differences of labels thus they are independent of the choice of integer to label the first arc of K , thus, the weights are well-defined. Notice that the associated flat diagram to the virtual closure of a knotoid is labeled as the same as the knotoid since virtual crossings do not add any new arcs or labels. In fact, we have $P_K(t) = P_{\bar{v}(K)}(t)$, for K is a knotoid diagram and $\bar{v}(K)$ is the virtual closure of K . The virtual closure map connects the first and the last arc of a knotoid diagram so these arcs are labeled with the same integer in the closure. Since the weights are well-defined up to this integer labeling, it is convenient to label both the first and the last arcs with 0.

Theorem 4.8. *The affine index polynomial is a virtual knotoid invariant.*

Proof. The polynomial P_K , by its definition, is independent of the moves generated by the detour move; involving the virtual Ω - moves and the partial virtual moves, also Ω_v - move. Thus it suffices to check the invariance under oriented $\Omega_{i=1,2,3}$ - moves. The integer labeling is uniquely inherited under these three moves so we check the local changes for the labels in the move patterns. Note that for the verification of oriented virtual knot invariants, it is sufficient to check two orientation types of the first move, one type of the second move and one type of the third move where there is a cyclic triangle in the middle and two of the crossings have the same sign and the third crossing has the opposite sign [30]. This verification holds for oriented knotoid invariants as well. We check these four types of oriented moves for the verification of the invariance of the affine index polynomial. Figure 31 depicts the verification. \square

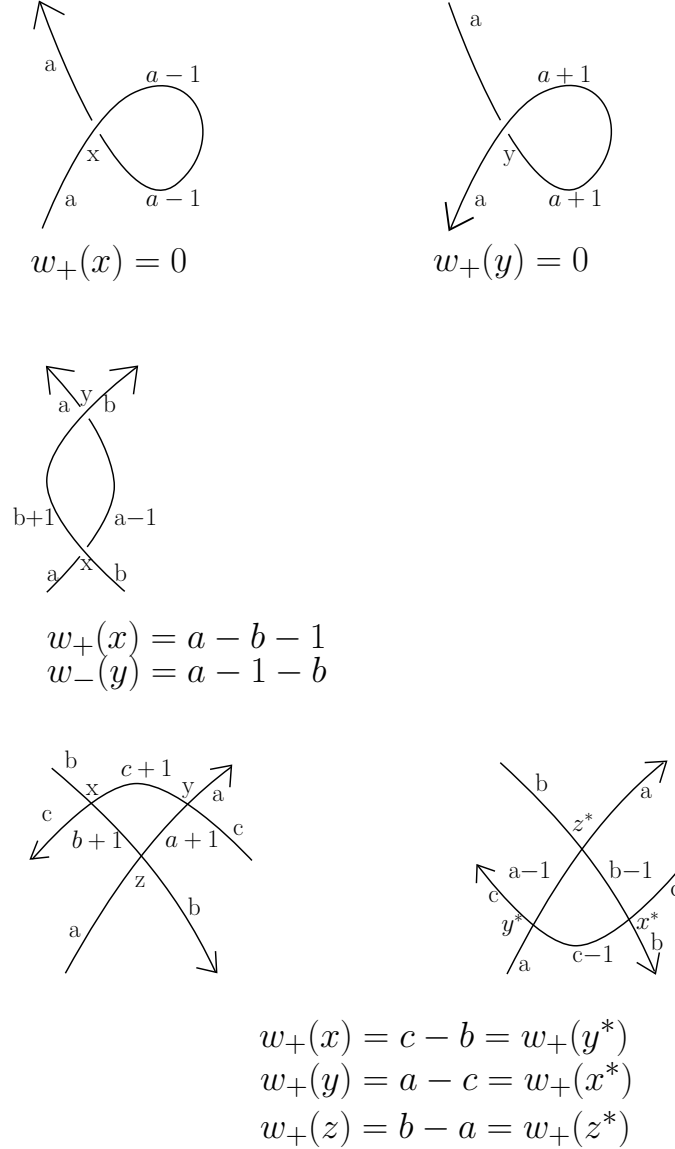


FIGURE 31. The invariance of the affine index polynomial under the oriented moves

Remark 5. The affine index polynomial is generalized to an invariant of virtual links by A.Cheng and H.Gao [4]. We will study generalizations of these invariants to classical and virtual multi-knotoids in a sequel to the present paper.

4.4. A comparison of affine index polynomials: Knotoids vs Knots. The affine index polynomial of a classical knotoid is the same as the affine index polynomial of its virtual closure knot. But the polynomial behaves differently for classical knotoids than it behaves for virtual knots in general.

- (1) Classical knotoids have nontrivial affine index polynomial although the polynomial is trivial for all classical knots. Having the same structure with classical knots, knot-type knotoids have trivial affine index polynomial. On the other hand, proper knotoids can have nontrivial affine index polynomial. This is used to determine whether

a knotoid is proper or knot-type knotoid. If a given classical knotoid diagram has nonzero affine index polynomial, then we can conclude that this knotoid diagram is in the class of a proper knotoid.

- (2) The *inverse* of an oriented virtual knot diagram is obtained by reversing the orientation of the diagram. For the affine index polynomial of a virtual knot k , we have

$$P_K(t) = P_{\overline{K}}(t^{-1}),$$

where K is an oriented diagram of k and \overline{K} is the inverse of K .

This can be used to distinguish a virtual knot from its inverse. The *inverse* of a knotoid diagram is defined in the same way by the reversion operation. The equality above does not hold for the affine index polynomial of classical knotoids, as we explain below.

Definition 10. The weights of crossings of a knotoid diagram K are said to be *symmetric* if for any classical crossing of K , c_1 with a nonzero positive weight $w_+(c_1)$, there is another classical crossing c_2 with a nonzero positive weight such that $w_+(c_2) = -w_+(c_1)$. These two crossings with opposite positive weights are said to be *paired* crossings.

Lemma 4.9. *The weights of the crossings of any flat classical knotoid diagram are symmetric.*

Proof. The proof relies on Proposition 3.6 which tells that all flat classical knotoid diagrams can be obtained from the trivial knotoid diagram by a finite sequence of the flat $\Omega_{i=1,2,3}$ -moves and also by isotopy of the 2-sphere. Using this fact, we will proceed by induction on the number of the flat $\Omega_{i=1,2,3}$ -moves applied to the trivial diagram.

The trivial diagram has no crossings so conventionally it satisfies the lemma.

Let's start with the diagrams shown in Figure 32, which are one or two Ω_i -moves away from the trivial knotoid diagram. As we see from the picture, the weights of crossings of these diagrams are symmetric. Let us assume that the weights of crossings of the flat classical knotoid diagrams which are $n > 0$ flat Ω_i -moves away from the trivial knotoid diagram are symmetric.

Suppose \tilde{K} is a flat knotoid diagram which is $n + 1$ flat Ω_i moves away from the trivial diagram. So it is one flat move away from an n move away flat knotoid diagram K .

The flat Ω_2 move adds two crossings to K with symmetric weights and this move does not make any change in the weight charts of other crossings. We know by the induction hypothesis that the other crossings of K are paired thus the weights of the crossings of the diagram \tilde{K} become symmetric by this move. The flat Ω_3 -move does not change the weights of the three crossings, A, B, C , located in the triangular region of the move. By the induction hypothesis we know that these three crossings of K are paired with some other crossings of K (either two of them with each other or with other crossings in the rest of the diagram). The weights of crossings in local move region and also in the rest of the diagram remain invariant under this move. Thus the weights of \tilde{K} are symmetric regardless of this move. The flat Ω_1 -move adds/removes one crossing with zero weight to the given diagram K so this move does not disturb the symmetry of weights. Therefore, the weights of the crossings of \tilde{K} are symmetric. This completes the induction and proves the lemma. \square

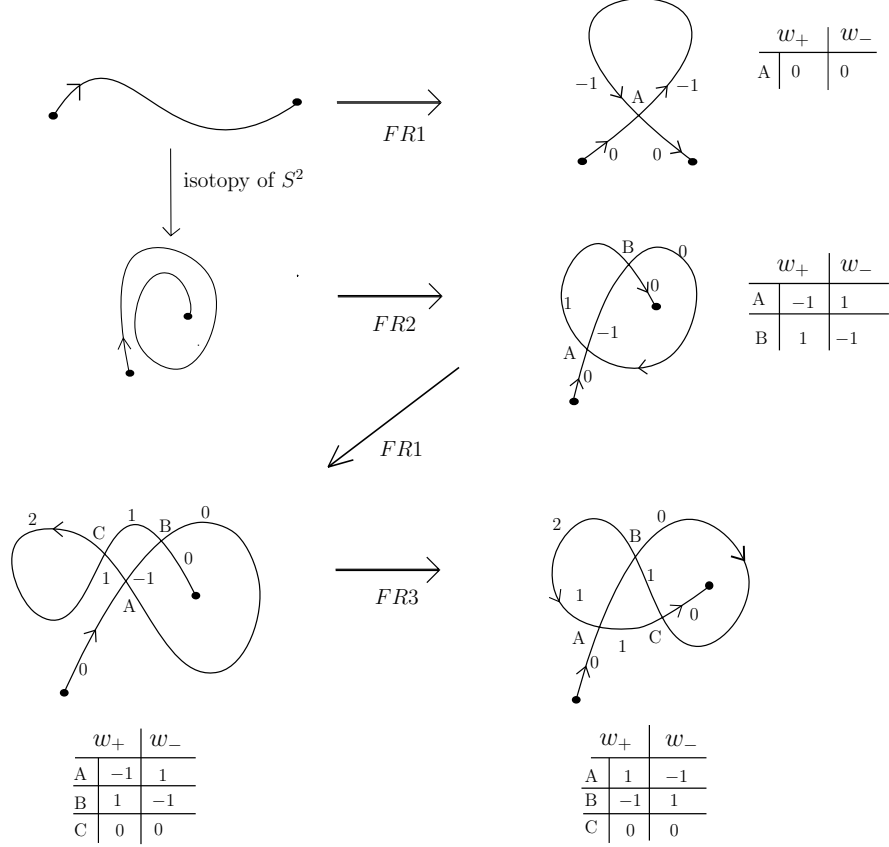


FIGURE 32. Induction step

Theorem 4.10. *The affine index polynomial of a classical knotoid is symmetric with respect to $t \leftrightarrow t^{-1}$, that is, $P_K(t) = P_{\bar{K}}(t)$.*

Proof. Lemma 4.9 shows that any crossing of a classical knotoid diagram with a nonzero positive weight is paired with another crossing. If the signs of paired crossings are different then the contributions cancel out each other and contribute to the affine index polynomial trivially. Let c_1 and c_2 be paired crossings both positive, then they contribute to the polynomial as the summands $(t^n - 1)$ and $(t^{-n} - 1)$, respectively, where n is the weight of c_1 and $-n$ is the weight of c_2 . Since any classical knotoid is represented by a classical knotoid diagram and the affine index polynomial is a classical knotoid invariant, the theorem follows. \square

Theorem 4.10 tells us that the affine index polynomial of knotoids fails in distinguishing a classical knotoid diagram from its inverse. However, there are virtual knotoids which do not satisfy Theorem 4.10. This may be useful for detecting the virtuality of knotoids. For instance, all the virtual knotoid diagrams overlying the flat diagram shown in Figure 33 have a non-symmetric affine index polynomial. Consequently, none of these virtual knotoid diagrams are virtually equivalent to a classical knotoid diagram and each of them represents a nontrivial virtual knotoid of genus one.

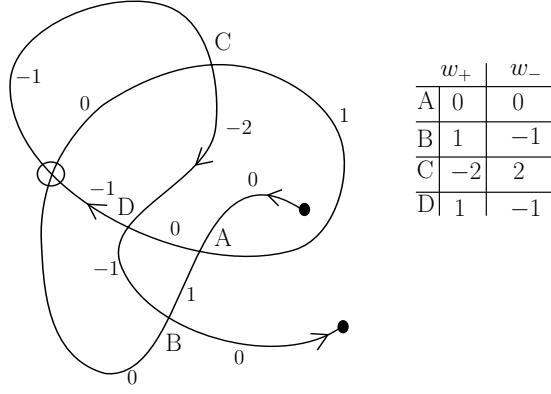


FIGURE 33. A flat virtual knotoid with non-symmetric weights

The symmetry of the affine index polynomial of classical knotoids gives rise to the following theorem.

Theorem 4.11. *If the affine index polynomial of a virtual knot is not symmetric with respect to $t \leftrightarrow t^{-1}$ then it is not a virtual closure of a classical knotoid K . In other words, it is not in the image of the virtual closure map \bar{v} .*

Proof. The proof follows from the equality $P_K(t) = P_{\bar{v}(K)}(t)$ and from Theorem 4.10. \square

4.5. Affine Index Polynomial and the Height of Knotoids. The *height* (or the complexity) of a classical knotoid diagram is the minimum number of crossings that a shortcut creates during the underpass closure. The *height of a classical knotoid K* is defined as the minimum of the heights, taken over all equivalent classical knotoid diagrams to K . The height is a classical knotoid invariant [34]. A classical knotoid is of knot-type if and only if its height is zero or equivalently a classical knotoid has nonzero height if and only if it is a proper knotoid [34].

It is often hard to compute the height with an attempt of direct computation for we should take into account all the equivalent knotoid diagrams. The affine index polynomial provides the following estimation for the height.

Theorem 4.12. *Let K be a classical knotoid and $|m|$ be the maximal weight of the crossings of K . If the maximum degree of the affine index polynomial of K is $|m|$ then the height of K , $h(K) \geq |m|$.*

Proof. Let C be one of the crossings of K with maximal weight $|m|$ and $l(C)$ be the loop associated with C . The weight of a crossing is either the difference of the entering label value and the exit label value of the loop associated to the crossing or the negative of this difference. The entering label can change while traversing the loop; it either increases or decreases by 1 each time when it meets a crossing on the loop, depending on the algebraic intersection number of the loop with the intersecting strand. If the entering value to the loop is a then the exit value is $a - n$ where n is the algebraic intersection number of the loop with the rest of the diagram. Therefore, the algebraic intersection number of $l(C)$ with the rest of the diagram is equal to either $w_-(C)$ or $w_+(C)$ due to the orientation; if the loop yields in the counterclockwise orientation then it is $w_-(C)$ otherwise it is $w_+(C)$ as seen in Figure 34.

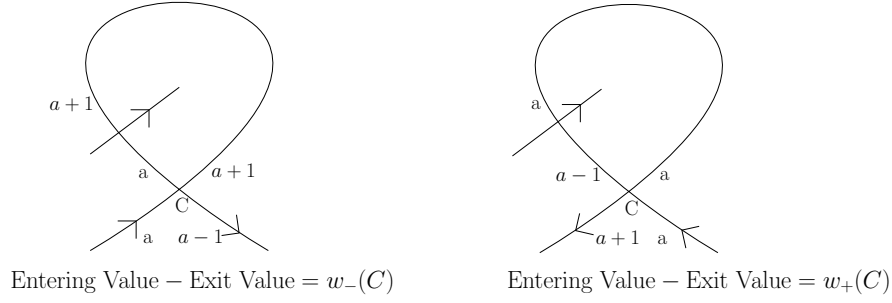


FIGURE 34. The weights with respect to the orientation of the loop at C

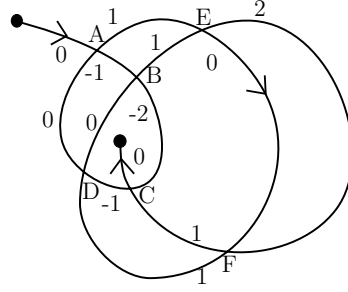
The smoothing of a classical crossing in an oriented way as pictured in Figure 35 is called *Seifert smoothing*. We apply the *Seifert smoothing* to all crossings which are met twice while traveling through the loop $l(C)$.



FIGURE 35. Seifert smoothing of a crossing

The Seifert smoothing of the crossing C results in oriented Seifert circles and an oriented long segment containing the endpoints. The algebraic intersection number of the Seifert circles which are nested around the endpoints with the long segment is denoted by I_K and is equal to the algebraic intersection number of the loop with the rest of the diagram, since none of the crossings that contribute nontrivially to this intersection number are smoothed during the Seifert smoothing. This shows that the algebraic intersection number of the Seifert circles with the long segment obtained by smoothing C , is equal to either $w_-(C)$ or $w_+(C)$.

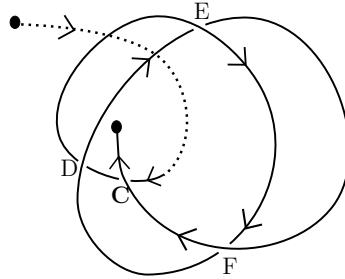
The number $|I_K|$ can be at most as large as the number of the Seifert circles nested around the endpoints. The height of the diagram K is at least as large as the number of Seifert circles, by the Jordan curve theorem. Thus we have the inequality $h(K) \geq |m|$, where $|m|$ is the maximal weight of the crossings of K . Since the affine index polynomial was a knotoid invariant, $|m|$ will appear as the maximal degree in the polynomial for any knotoid diagram equivalent to K meaning that there will be a crossing with weight $|m|$ in each representative knotoid diagram. This gives us the inequality, $h(K) \geq |m|$ and completes the proof. Figure 36 gives an illustration for the proof on the knotoid diagram K in Figure 1g. \square



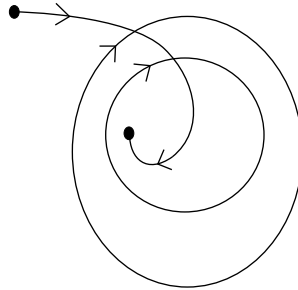
	w_+	w_-
A	$\begin{pmatrix} -1 \\ 1 \end{pmatrix}$	1
B	$\begin{pmatrix} -2 \\ 2 \end{pmatrix}$	2
C	$\begin{pmatrix} 2 \\ -2 \end{pmatrix}$	-2
D	$\begin{pmatrix} 1 \\ 1 \end{pmatrix}$	-1
E	$\begin{pmatrix} 1 \\ 1 \end{pmatrix}$	1
F	$\begin{pmatrix} 1 \\ 1 \end{pmatrix}$	-1

$$P_K(t) = t^2 + t + t^{-1} + t^{-2} - 6$$

(a) $F(K)$ with integer labels



(b) Loop of the crossing C



(c) Seifert circles and the long segment

FIGURE 36. An illustration for the proof of Theorem 4.12

One immediate consequence of Theorem 4.12 is that we are able to tell the height of the knotoids given with a spiral diagram with all the crossings are positive. In particular, the heights of the knotoids overlying the flat diagrams given in Figure 37 are 1, 2 and 3, respectively, when all crossings are chosen to be positive. This is generalized as follows. The affine index polynomial of the classical knotoid represented by an n -fold spiral knotoid diagram has a term of the form $t^n + t^{-n}$ if all crossings of the diagram are positive. The maximal degree of the affine index polynomial is n and the height of the spiral diagram is

n then by Theorem 4.12, the height of the knotoid is n . Thus we have an infinite set of knotoids whose height is given by the affine index polynomial.

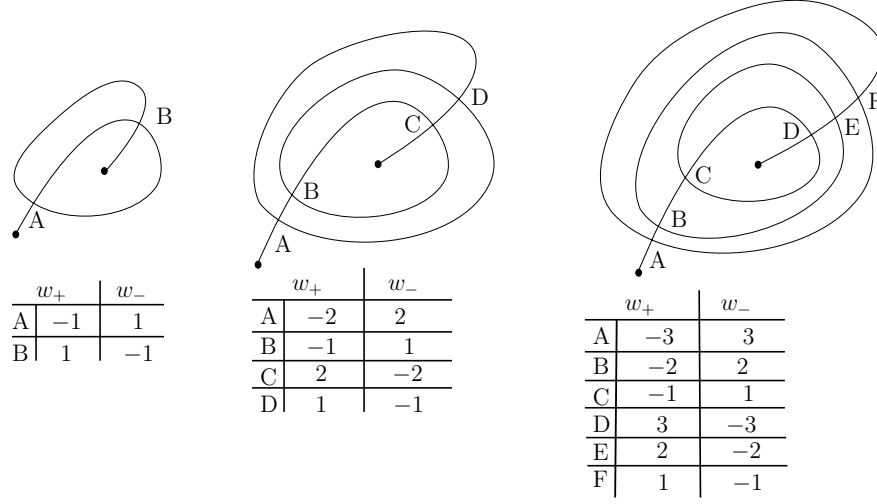


FIGURE 37. Flat spiral knotoid diagrams

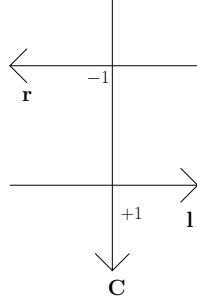
But there are examples of nontrivial proper knotoids with trivial affine index polynomial so that the polynomial is giving trivial lower bound for the height of knotoids. For instance, for overlying diagrams of the above flat diagrams, if some of the crossings are chosen to be negative crossings, the affine index polynomial is trivialized. In particular, choose the crossings B , C and D negative and A , E , F positive crossings for overlying the third flat diagram above. The affine index polynomial of the represented knotoid is zero in this case. This reveals the following question: *Are there any other knotoid invariants giving any nontrivial information about the height?* The arrow polynomial which will be discussed in the following section gives an answer to this question. But first, we make a small note on Z. Cheng's generalization of the affine index polynomial of virtual knots [3].

4.6. Cheng's Generalization of the Affine Index Polynomial. The two variable polynomial $F_K(t, s)$ is defined by utilizing the weights of crossings and algebraic intersection numbers of chords in the chord diagram of K . It is an invariant of virtual knots and can be defined in the same way for virtual knotoids. The chord diagrams of knotoid diagrams illustrate the intersection numbers directly in the patterns of intersection numbers of chords. The weight of a crossing is equal to the algebraic intersection number of the chord of the crossing with other chords; $w_K(c) = r_+ - r_- - l_+ + l_-$, where $r_+(r_-)$ is the number of positive chords crossing the chord of c from left to right (negative chords, respectively) and $l_+(l_-)$ is the number of negative crossings crossing the chord of c from right to left (negative chords, respectively). In particular, for the knotoid diagram \tilde{K} in Figure 38b we have the equality,

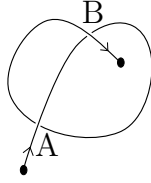
$$\begin{aligned} w_{\tilde{K}}(A) &= A \cdot B = -1 \\ w_{\tilde{K}}(B) &= B \cdot A = +1 \end{aligned}$$

where $A \cdot B$ is the algebraic intersection number of A with B and $B \cdot A$, the algebraic intersection number of B with A . Note that the choice of the right and the left of our use which is also given in Figure 38a, is the opposite of Cheng's convention for the right and the left. As

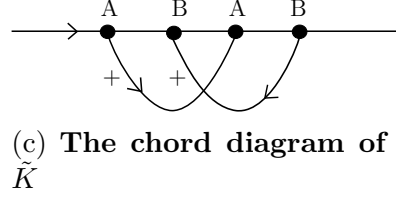
a result, the algebraic intersection number of our convention is not the usual right-handed algebraic intersection number.



(a) Convention for right and left



(b) The knotoid diagram \tilde{K}



(c) The chord diagram of \tilde{K}

FIGURE 38

Definition 11. Let K be a virtual knotoid diagram. The *index function* of a classical crossing c , $g_c(s)$ is defined by utilizing the intersections of chords with the chord of c as follows:

$$g_c(s) = \sum_i \text{sgn}(r_i) s^{\overline{w_K(r_i)}} - \sum_j \text{sgn}(l_j) s^{\overline{-w_K(l_j)}}$$

where the sums are taken over all right going and left going chords crossing the chord of c respectively, $\text{sgn}(r_i), \text{sgn}(l_j)$ are the signs of the corresponding crossings to r_i and l_j , $\overline{w_K(r_i)} = w_K(r_i) \pmod{|w_K(c)|}$ and $\overline{-w_K(l_j)} = -w_K(l_j) \pmod{|w_K(c)|}$ for $w_K(c)$ is the weight of c .

The polynomial $F_K(t, s)$ is defined as

$$F_K(t, s) = \sum_{c_i} \text{sgn}(c_i) t^{g_{c_i}(s)} - \text{wr}(K)$$

where $\text{wr}(K)$ is the writhe of K .

$F_K(t, s)$ is a virtual knotoid invariant. The verification of the invariance of $F_K(t, s)$ for virtual knotoids follows the same as the verification of the invariance of the polynomial for virtual knots, the reader is directed to [3] for details. We shall refer to $F_K(t, s)$ as the Cheng polynomial. The Cheng polynomial generalizes the affine index polynomial. For K a knotoid, it can be seen that

$$F_K(t, 1) = P_K(t).$$

Example 4.1. The overlying diagram of the spiral knotoid diagram given on the right in Figure 37 with crossings A, E, F positive and B, C, D negative has a chord diagram as shown in Figure 39. This knotoid diagram K has trivial Cheng polynomial $F_K(t, s)$ as well as trivial affine index polynomial.

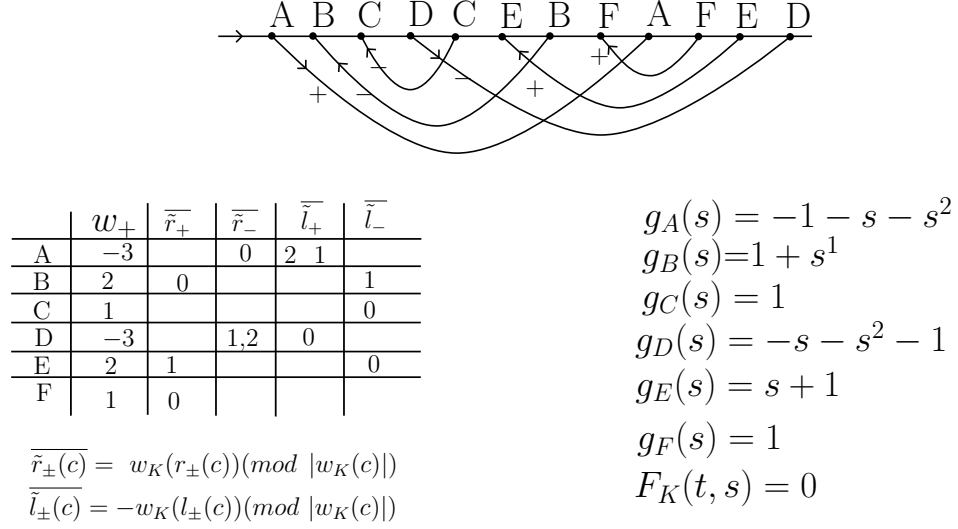


FIGURE 39. The Cheng polynomial of the overlying diagram of the spiral diagram in Figure 37

It is of interest that $F_K(t, s)$ is trivial in this case. Clearly there is much more to be done in investigating the Cheng polynomial for knotoids. In the next section we will detect this example with a different invariant of knotoids, the arrow polynomial.

5. THE ARROW POLYNOMIAL

We define the arrow polynomial for knotoids in analogy with the arrow polynomial of virtual knots and links which was defined by H.A. Dye and L.H. Kauffman [DK] and independently by Y. Miyazawa [28]. The construction of the arrow polynomial of knotoids both for classical and virtual is based on the *oriented state expansion* of the bracket polynomial of knotoids which is shown in Figure 40.

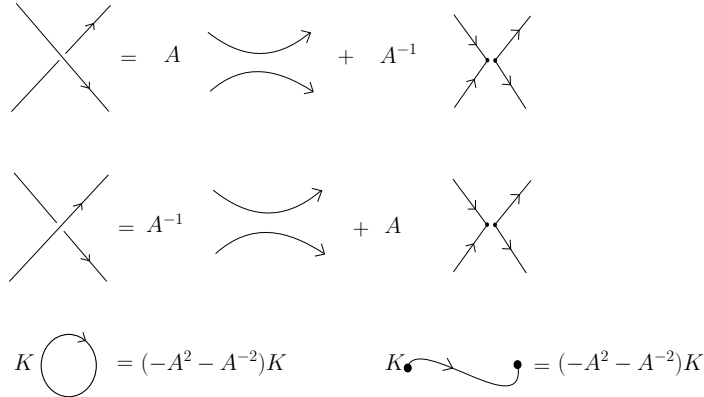


FIGURE 40. Oriented state expansion

Oriented state expansion of knotoids involves *oriented and disoriented smoothings* of classical crossings which are resulted in *oriented states* with circular components and one long state component or a single long state component. The state components obtained by disoriented smoothings include an extra combinatorial structure in the form of *paired cusps*. Each cusp has two arcs either going into the cusp or two arcs going out from the cusp. A cusp can be denoted by an angle which locally divides S^2 into two parts. One part is the span of the acute angle and the other part is the span of the obtuse angle. We call the part which is the span of the acute angle as *inside* of the cusp and the part which is the span of the obtuse angle as *outside* of the cusp.

All state components of a virtual knotoid diagram are taken under the virtual equivalence which is generated by the isotopy of S^2 and the detour move and there is a list of rules shown in Figure 41 to reduce the number of cusps in a state component which are set accordingly with the invariance under $\Omega_{i=1,2,3}$ -moves. The basic reduction rule consists of cancellation of two consecutive cusps both with insides on the same side of the segment connecting them. Two consecutive cusps on a state component which have insides on the opposite sides of the segment connecting them, are not canceled out. Specifically, any two consecutive cusps on a circular component are canceled if they have insides in the same local region that the circle forms. Therefore, a circular component with two such cusps turns into an embedded circular component which contributes to the polynomial as $d = (-A^2 - A^{-2})$. Any two consecutive cusps on a long state which have insides on the same side of the segment connecting them, are canceled out as well. The long state turns into an embedded arc in S^2 and contributes to the polynomial with the same value of an embedded circular state, as $d = (-A^2 - A^{-2})$. Two cusps on a circular component with insides on the opposite local sides of the circle remain as graphical nodes. This component is regarded as a circular graph state. The long state component with surviving cusps (cusps with insides on opposite sides of the connecting segment) is regarded as a graphical state as well. The graphical components contribute to the polynomial as extra variables. A circular graph component with surviving cusps can be turned into a circular graph without any virtual crossings by the detour move so that it can be depicted as a circular graph with cusps forming zig-zags on the component. A circular component with two cusps forming a zig-zag contributes as K_1 to the polynomial. In general, a circular graph with zig-zags formed by $2i$ alternating cusps, contributes as a variable, K_i to the arrow polynomial. A long state component with i zig-zags that is formed by alternating cusps contributes as an additional variable, as Λ_i to the arrow polynomial.

Definition 12. We define the *arrow polynomial* of a knotoid diagram K as,

$$A[K] = \sum_S \langle K|S \rangle (-A^2 - A^{-2})^{\|S\|-1} \langle \hat{S} \rangle$$

where the sum runs over the oriented bracket states, $\langle K|S \rangle$ is the usual vertex weights of the bracket polynomial, $\|S\|$ is the number of components of the state S and $\langle \hat{S} \rangle$ is the product of variables, $K_{i_1}^{j_1} \dots K_{i_n}^{j_n} \Lambda_i$, associated to the components of S with surviving cusps; K_i to the circular ones and Λ_i to the long segment component.

The variables K_i and Λ_i constitute an infinite set of commuting variables, commuting with each other also with the variable A of the arrow polynomial. Ω_1 - move changes the arrow polynomial in the same way it changes the bracket polynomial of knotoids. Multiplication

with $(-A^3)^{-\text{wr}(K)}$, where $\text{wr}(K)$ is the writhe of K normalizes the arrow polynomial and turns it into a virtual knotoid invariant.

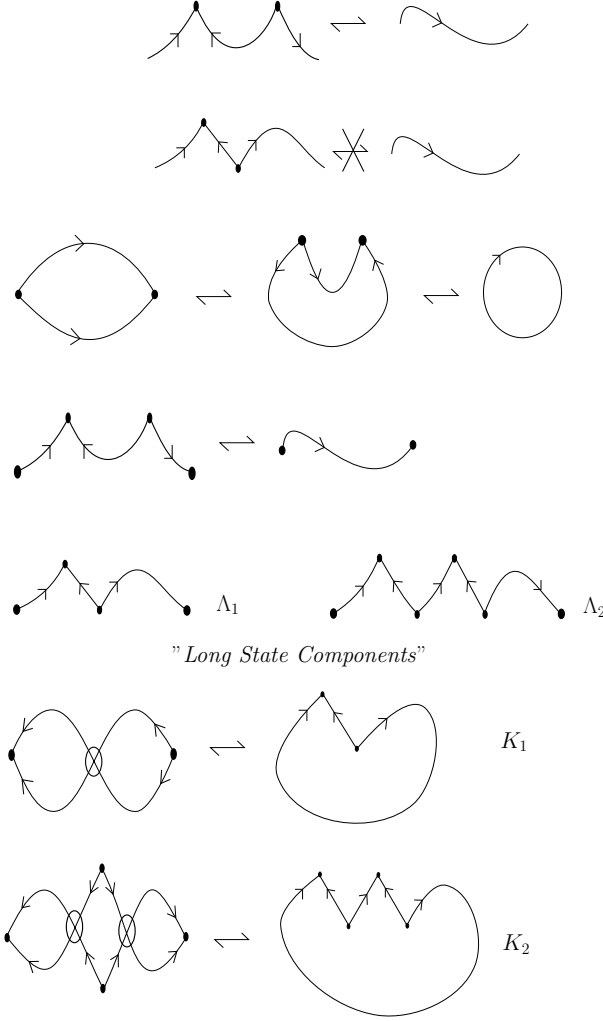


FIGURE 41. Reduction rules for the arrow polynomial

Theorem 5.1. *The normalized arrow polynomial is a virtual knotoid invariant.*

Proof. The proof follows the same as the proof of the invariance of the arrow polynomial for virtual knots/links. See [8]. \square

Definition 13. The K -degree of a summand of the arrow polynomial of a virtual knotoid which is of the form, $A^m(K_{i_1}^{j_1} K_{i_2}^{j_2} \dots K_{i_n}^{j_n}) \Lambda_k$ is equal to

$$i_1 \times j_1 + \dots i_n \times j_n.$$

The K -degree of the arrow polynomial of a virtual knotoid is the maximum K -degree of the polynomial. Note that the K -degree of the arrow polynomial of a virtual knot/link is defined in similar way, as the maximum K -degree of the polynomial [8].

Definition 14. The Λ -degree of a summand of the arrow polynomial is equal to the half of the number of irreducible cusps in the corresponding long state component. For the

summand form given above, Λ -degree is equal to k . The Λ -degree of the arrow polynomial of a virtual knotoid is the maximum Λ -degree of the polynomial.

Note that instead of Λ_i , we could assign K_i as a variable to long state components with $2i$ surviving cusps then we would have

$$A[K] = A[\bar{v}(K)],$$

for any virtual knotoid K .

However, assigning Λ_i to the long state components with $2i$ surviving cusps the arrow polynomial turns into more powerful invariant for knotoids. Figure 42 depicts the oriented state expansion of the knotoid represented in Figure 21. The arrow polynomial of the virtual closure of this knotoid is trivial. The non-triviality of the knotoid is detected by assigning Λ_i to the long state components. Another example is the following virtual knotoid shown in Figure 43. The virtual closure of this knotoid is the Slavik's Knot [8] whose normalized arrow polynomial is trivial. But the arrow polynomial of the knotoid with Λ_i -variables is nontrivial, $A[K] = A^{-9} + A^{-7} + 3A^{-5} + 3A^{-3} - A^3(-6 + \Lambda_1) - A^{-1}(-5 + \Lambda_1) + A^{-3}\Lambda_1 + A(1 + \Lambda_1) + A^5(2 + \Lambda_1)$. Then it is a nontrivial virtual knotoid.

$$\begin{aligned}
 A[\text{Diagram}] &= A^2 \text{Diagram}_1 + A A^{-1} \text{Diagram}_2 \\
 &+ A^{-1} A \text{Diagram}_3 + A^{-2} \text{Diagram}_4 \\
 &= (A^2 + A^{-2}) \Lambda_1 + (-A^2 - A^{-2}) K_1 + 1
 \end{aligned}$$

FIGURE 42. The arrow polynomial of the knotoid in Figure 21

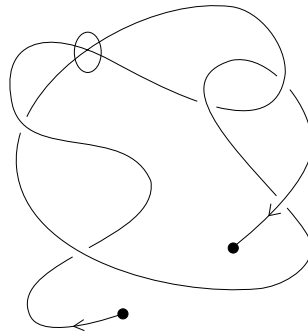


FIGURE 43. The knotoid closing to Slavik's knot

Theorem 5.2 ([13]). *In a classical knot or link diagram, all state components of the arrow polynomial reduce to loops that are free from cusps.*

The virtual closure of a knot-type knotoid diagram is a classical knot diagram. Thus the oriented state components of a knot-type knotoid diagram turn into the oriented state components of a classical knot diagram when the endpoints of long components are connected virtually. Then it follows from the above theorem that cusps do not survive in any of the state components of a knot-type knotoid diagram and the arrow polynomial is in fact the usual bracket polynomial of the knotoid represented. This conclusion can be used to tell about the type of a given knotoid diagram. In fact, if the K - or the Λ -degree of the arrow polynomial of a knotoid is nonzero then it is immediate to conclude that it is not a knot-type knotoid. For proper knotoid diagrams, cusps can survive only on the long segment component of states. The reason that the circular components are free of cusps is the same as the reason for the non-existence of cusps in the states of classical knot diagrams. As a conclusion, the K -degree of the arrow polynomial of a classical knotoid is zero. For virtual knotoids, cusps can survive in circular state components as well as they can survive in long state components which means that both the K - and Λ -degrees of the arrow polynomial of a virtual knotoid may be nontrivial. We can conclude that the knotoid in Figure 42 is a non-classical knotoid since the K -degree of the arrow polynomial is 1.

Remark 6. For K_1 and K_2 in Figure 22, $A[K_1] = 1 - A^{-4} + A^4 - \Lambda_1 A^{-2} + A^2 \Lambda_1$ and $A[K_2] = 2 - A^{-4} - A^4 + A^8 - \Lambda_1 A^{-6} + \Lambda_1 A^{-2}$. Therefore K_1 is not equivalent to K_2 .

Remark 7. The arrow polynomial generalizes to a virtual multi-knotoid invariant directly: All crossings including the crossings shared by two components of a given oriented virtual multi-knotoid diagram are smoothed in the same way. We sum over the resulted oriented state components which are labeled by A or A^{-1} at each smoothing site and we have the arrow polynomial for multi-knotoids.

If K is a multi-knotoid diagram without any virtual crossings then it is obvious that the circular components of K are free of cusps, and cusps can survive only on the long segment component.

5.1. The Arrow Polynomial and the Height of Knotoids. In addition to determining non-triviality and the type of a knotoid, the arrow polynomial can be used for estimating the height of a classical knotoid. Let us recall some more facts from virtual knot theory.

Definition 15. The *virtual crossing number* of a virtual knot/link is the minimum number of virtual crossings over all representative diagrams.

The problem of determining the virtual crossing number of a virtual knot or link is a fundamental problem in virtual knot theory. There is a relation between the virtual crossing number and the maximal K -degree of the arrow polynomial of a virtual knot, as stated by the following theorem.

Theorem 5.3. [8] *The virtual crossing number of a virtual knot/link is greater or equal to the maximal K -degree of the arrow polynomial of that virtual knot/link.*

Closing a classical knotoid virtually has an effect on the states of the arrow polynomial as closing the endpoints of the long state components in the virtual fashion. Therefore the

Λ_i -variables assigned to long state components with surviving cusps of a knotoid transform to K_i -variables assigned to the circular components with surviving cusps in the arrow polynomial of the virtual knot which is the virtual closure of the knotoid. Using this idea, we show that for classical knotoids, the Λ -degree of the arrow polynomial of a classical knotoid can be used as a lower bound for the height.

Theorem 5.4. *The height of a classical knotoid K is greater than or equal to the Λ -degree of its arrow polynomial.*

Proof. Let \tilde{K} be a classical knotoid diagram representing K . By Theorem 5.3 and the discussion above we have the following inequality,

$$\text{The } \Lambda\text{-degree of } A[K] \leq \text{the virtual crossing number of the knot } \bar{v}(K)$$

The least number of virtual crossings obtained by closing a classical knotoid diagram virtually, is equal to the height of that diagram. Then,

$$\text{The } \Lambda\text{-degree of } A[K] \leq h(\tilde{K}),$$

where $h(\tilde{K})$ is the height of the knotoid diagram \tilde{K} . The inequality above holds for any classical knotoid diagram equivalent to K since the Λ -degree of the polynomial is invariant under $\Omega_{i=1,2,3}$ -moves. Therefore we have,

$$\text{The } \Lambda\text{-degree of } A[K] \leq \text{the height of } K.$$

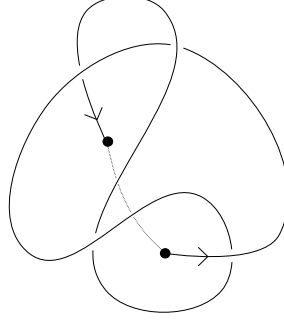
□

Thus we have two tools; the affine index polynomial and the arrow polynomial for estimating the height of a classical knotoid. There are cases that both of the polynomials give the height and there are cases that one of the polynomials give a more accurate estimation. We show some examples for each of these cases.

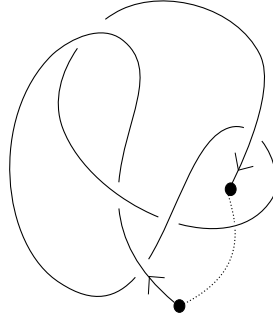
Example 5.1. The affine index polynomial of the knotoid that is overlying the flat knotoid diagram given in Figure 37 is trivial when the crossings B , C and D are chosen to be negative and the other crossings to be positive. But the arrow polynomial of the knotoid is nontrivial, $A[K] = -A^{-6}\Lambda_1 - 2A^{-4}\Lambda_2 - 2A^4\Lambda_2 + (1 + 4\Lambda_2) - A^{-6}\Lambda_3 + A^{-2}(\Lambda_1 + \Lambda_3) + A^2(\Lambda_1 + \Lambda_3) - A^6(\Lambda_1 + \Lambda_3)$. The Λ -degree of the arrow polynomial is 3 so the arrow polynomial gives a nontrivial lower bound for the height. We can see that the height of the given diagram is also 3. Thus the height of the knotoid represented is 3.

Example 5.2. Figure 44a and 44b shows the knotoid 4.8 and the knotoid 5.7 [1], respectively. Both knotoid 4.8 and 5.7 are classical knotoids with trivial odd writhe and trivial affine index polynomial. However, the arrow polynomials of the knotoids are nontrivial. $A[K_{4.8}] = \Lambda_1 + A^{-8}\Lambda_1 - 2A^{-4}\Lambda_1 - A^{-2}\Lambda_2 + A^2(1 + \Lambda_2)$. This tells us that the height of the knotoid 4.8 is at least 2 and the knotoid diagram given has height 2. We can conclude that the knotoid 4.8 is a nontrivial proper knotoid with height 2.

Also, $A[K_{5.7}] = -A^{-3} + A - 2A^5 + A^9 + A^{-9}\Lambda_1 - 2A^{-5}\Lambda_1 + 2A^{-1}\Lambda_1 - 2A^3\Lambda_1 + A^7\Lambda_1$. So the height of the given knotoid is at least 1 and in fact, from the diagram given, we see that the height of the diagram is 1. Therefore the height of the knotoid 5.7 is 1.



(a) The knotoid 4.8



(b) The knotoid 5.7

FIGURE 44

Example 5.3. The arrow polynomial of the knotoid represented by the diagram in Figure 1g is $A[K] = A^6 - A^{-4}\Lambda_1 + A^4\Lambda_1 - A^{-2}\Lambda_2 + A^2\Lambda_2$. Thus the Λ -degree of the polynomial is 2. We computed the affine index polynomial in the previous section and saw that the maximal degree of the polynomial is also equal to 2. So both the affine index polynomial and the arrow polynomial give the same lower bound for the height. The height of the given diagram is 2. Therefore the height of the knotoid represented is 2.

Example 5.4. We see that the height of the knotoid diagram given in Figure 1f is equal to 2. But we want to find out if there exists an equivalent knotoid diagram with less height. The affine index polynomial and the arrow polynomial of the knotoid assure that the height is at least 1. In fact, $P_K(t) = 2t + 2t^{-1} - 4$ and $A[K] = -A^{-5} + 2A^{-1} - A^3 - A^7 + 2A\Lambda_1 - 2A^5\Lambda_1$ so that we are able to say that the knotoid given by this diagram is a proper knotoid. But what is the height of the knotoid, is it 1 or 2?: With our tools discussed in this paper we can not give the answer of this question.

6. DISCUSSION

We end the paper with a full list of the questions that are discussed throughout the paper and possible future directions for the study of knotoids.

- (1) Determination of the kernel of the virtual closure map: We have nontrivial virtual knotoids closing virtually to the trivial knot. For a knot-type knotoid K , the virtual closure of K holds the same structure with K . Therefore, nontrivial knot-type knotoids close to nontrivial knots. *Is there a proper knotoid (a classical knotoid with nonzero height) whose virtual closure is the trivial knot?*

- (2) Determination of the image of the virtual closure map: *How to determine if a given virtual knot is in the image of \bar{v} or not? Is the virtual closure map surjective?*
- (3) A generalization of the first question: *Is there a proper knotoid whose virtual closure is a classical knot or do proper knotoids always close (virtually) to a virtual knot of genus 1?*
- (4) A generalization of the Jones polynomial conjecture: *The Jones polynomial for knotoids in S^2 detects the triviality of classical knotoids.* Let \bar{K} be a virtual knot with trivial Jones polynomial. If the conjecture holds, we will be able to conclude that the virtual closure of any proper knotoid is nontrivial, by using the equality $J(K) = J(\bar{v}(K))$. Also, there are virtual knots which are candidates to be in the image of \bar{v} for being genus 1 virtual knots. One of them is given in Figure 20 in Section 3.3. This virtual knot (listed in [9] as the knot 3.1) is known to be nontrivial but it has trivial Jones polynomial. Assuming the conjecture for the Jones polynomial holds, we can conclude that this virtual knot is not the virtual closure of a classical knotoid.
- (5) We want to know more about the height of knotoids and its relations with both the affine index polynomial and the arrow polynomial. We have given examples where the estimation of the arrow polynomial is more powerful than the affine index polynomial in detecting the height of a given classical knotoid. Does there exist an example for which the index polynomial is superior to the arrow polynomial in height determination?
- (6) Khovanov homology can be extended to an invariant of knotoids. There is a direct analog of Khovanov homology for classical knotoids. The analogs of Khovanov homology for virtual knots [7, 27] can be applied to virtual knotoids. It is worth investigating Khovanov homology for knotoids. We can ask the following question: *Does Khovanov homology for knotoids detect the trivial knotoid?* Note that Khovanov homology detects the unknot [19].
- (7) Let C be an open oriented curve in 3-dimensional space. The set of knotoids associated to C that are obtained by projecting the curve to planes deserves more study since the physical properties of the curve can be studied in this way.

REFERENCES

- [1] A. Bartholomew, *Andrew Bartholomew's Mathematics Page: Knotoids*, <http://www.layer8.co.uk/maths/knotoids/index.htm>, January 14, 2015
- [2] J. Scott Carter and S. Kamada and M. Saito, *Stable Equivalence of Knots and Virtual Knot Cobordisms*, Knots 2000 Korea, Vol. 1 (Yongpyong). J. Knot Theory Ramifications, **11**, (2002), no. 3, 311-322
- [3] Z. Cheng, *A transcendental invariant of virtual knots*, arXiv:1511.08459v1 [math.GT], (26 Nov 2015)
- [4] Z. Cheng and H. Gao, *A polynomial invariant of virtual links*, J. Knot Theory Ramifications, **22**, (2013), no:12, 33 pp.
- [5] S. Chumutov and S. Duzhin and J. Mostovoy, *Introduction to Vassiliev Knot Invariants*, Cambridge University Press, Cambridge, (2012)
- [6] M. Dennis, *private conversation*, HH Wills Physics Laboratory, University of Bristol, UK

- [7] H.A. Dye and A. Kaestner and L.H. Kauffman, *Khovanov Homology, Lee Homology and a Rasmussen Invariant for Virtual Knots* (to appear in Journal of Knot Theory and Ramifications)
- [8] H.A. Dye and L.H. Kauffman, *Virtual Crossing Number and the Arrow Polynomial*, J. Knot Theory Ramifications, **18**, (2009), no.10, 1335-1357
- [9] J. Green, *A table of Virtual Knots*, <https://www.math.toronto.edu/drornb/Students/GreenJ/>, August 10, 2004
- [10] A. Kaestner, *On Applications of Parity in Virtual Knot Theory*, PhD thesis, University of Illinois at Chicago, USA, (2011)
- [11] A. Kaestner and L.H. Kauffman, *Parity, Skein Polynomials and Categorification*, Journal of Knot Theory and Its Ramifications, **21**, (10/2011), no.13, 56 pp.
- [12] L.H. Kauffman, *Virtual Knot Theory*, European Journal of Combinatorics, **20**, (1999), 663-690
- [13] L.H. Kauffman, *Introduction to Virtual Knot Theory*, J. Knot Theory Ramifications, **21**, (2012), no.13, 37 pp.
- [14] L.H.Kauffman, *Detecting virtual knots*, Atti. Sem. Mat. Fis. Univ. Modena, **49**, (Suppl.), (2001), 241-282
- [15] L.H.Kauffman, *Knot Diagrammatics*, Handbook of Knot Theory, edited by W.Menasco and M.Thistlethwaite, Elsevier B. V., Amsterdam, (2005), 233-318
- [16] L.H. Kauffman, *Knots and Physics*, Fourth edition, Series on Knots and Everything, **53**, World Scientific Publishing Co. Pte. Ltd., Hackensack, NJ, (2013), xviii+846 pp.
- [17] L.H. Kauffman, *An affine index polynomial invariant of virtual knots*, Journal of Knot Theory and Its Ramifications, **22**, (2013), no.4, 30 pp.
- [18] L.H. Kauffman, *New Invariants in the Theory of Knots*, Amer. Math. Monthly, **95**, (1988), 195-242
- [19] L.H. Kauffman and V. Manturov, *Virtual Biquandles*, Fund. Math., **188**, (2005), 103-146
- [20] A. Kawauchi, *A Survey of Knot Theory*, Birkhäuser Verlag,Basel, (1996)
- [21] P.B. Kronheimer and T.S. Mrowka, *Khovanov Homology is an Unknot Detector*, Publications mathématiques de l'IHS, **113**, June 2011, , Issue 1, pp. 97-
- [22] G. Kuperberg, *What is a Virtual Link?*, Algebraic&Geometric Topology, **3**, (2003), 587-591
- [23] C. Livingston and J.C. Cha, *A table of Knot Invariants*, <http://www.indiana.edu/~knotinfo/>
- [24] V. O. Manturov, *Parity in knot theory*, (Russian) Mat. Sb., **201**, (2010), no.5, 65-110; translation in Sb. Math., **201**, (2010), no. 5, 693-733
- [25] V. O. Manturov, *Knot Theory*, Chapman & Hall/ CRC Press, Boca Raton, FL, (2004)
- [26] V. O. Manturov, *Long Virtual Knots and Their Invariants*, J. Knot Theory Ramifications, **13**, (2004),1029-1039
- [27] V.O. Manturov and D.P.Ilyutko, *The State of Art: Virtual Knots*, Series on Knots and Everything:**51**, World Scientific Publishing Co.Pte. Ltd., Hackensack, NJ, (2013)
- [28] Y. Miyazawa, *A multivariable polynomial invariant for unoriented virtual knots and links*, Journal of Knot Theory and Its Ramifications, **17**, (2008), no.11, 1311-1326
- [29] S. Nelson, *Unknotting virtual knots with Gauss diagram forbidden moves*, J. Knot Theory Ramifications, **10**, (2001), no.6, 931-935.
- [30] M. Polyak, *Minimal Generating Sets Of Reidemeister Moves*, Quantum Topology, **1**, (2010), 399-411
- [31] R. C. Read and P.Rosenstiehl, *On the Gauss crossing problem* Combinatorics (Proc. Fifth Hungarian Colloq., Keszthely, (1976), Vol.**II**, 843-876, Colloq. Math. Soc. Janos Bolyai, **18**, North-Holland, Amsterdam-New York
- [32] C. Rourke, *What is a welded link?*, Intelligence of low dimensional topology, (2006), 263-270, Ser. Knots Everything, **40**, World Sci. Publ., Hackensack, NJ, (2007)
- [33] S. Satoh, *Virtual knot presentation of ribbon torus-knots*, J. Knot Theory Ramifications, **9**, (2000), no. 4, 531-542.
- [34] V. Turaev, *Knotoids*, Osaka Journal of Mathematics, **49**, (2012), no.1 195-223
- [35] V.A. Vassiliev, *Cohomology of knot spaces*, Theory of singularities and its applications, Adv. Soviet Math.,**1**, Amer. Math. Soc., Providence, RI, (1990), 23-69

LOUIS H.KAUFFMAN:DEPARTMENT OF MATHEMATICS, STATISTICS AND COMPUTER SCIENCE, UNIVERSITY OF ILLINOIS AT CHICAGO, 851 SOUTH MORGAN ST., CHICAGO IL 60607-7045, U.S.A.

E-mail address: nesli@central.ntua.gr

E-mail address: kauffman@math.uic.edu